MyoD regulates apoptosis of myoblasts through microRNA-mediated down-regulation of Pax3

Hiroyuki Hirai,[1,2,3] Mayank Verma,[1,2,3] Shuichi Watanabe,[1,2,3] Christopher Tastad,[1,2,3] Yoko Asakura,[1,2,3] and Atsushi Asakura[1,2,3]

[1]Stem Cell Institute, [2]Paul and Sheila Wellstone Muscular Dystrophy Center, and [3]Department of Neurology, University of Minnesota Medical School, Minneapolis, MN 55455

The molecules that regulate the apoptosis cascade are also involved in differentiation and syncytial fusion in skeletal muscle. MyoD is a myogenic transcription factor that plays essential roles in muscle differentiation. We noticed that *MyoD*$^{-/-}$ myoblasts display remarkable resistance to apoptosis by down-regulation of miR-1 (microRNA-1) and miR-206 and by up-regulation of Pax3. This resulted in transcriptional activation of antiapoptotic factors Bcl-2 and Bcl-xL. Forced *MyoD* expression induces up-regulation of miR-1 and miR-206 and down-regulation of Pax3, Bcl-2, and Bcl-xL along with increased apoptosis in *MyoD*$^{-/-}$ myoblasts. In contrast, *MyoD* gene knockdown increases cell survival of wild-type myoblasts. The 3′ untranslated region of Pax3 mRNA contains two conserved miR-1/miR-206–binding sites, which are required for targeting of these microRNAs (miRNAs). Therefore, these data suggest that MyoD not only regulates terminal differentiation but also apoptosis through miRNA-mediated down-regulation of Pax3. Finally, MyoD, miR-1, and miR-206 are all down-regulated in quiescent satellite cells, which may be required for maintenance of muscle stem cells.

Introduction

Adult skeletal muscle possesses extraordinary regeneration capabilities. After exercise or muscle injury, large numbers of new muscle fibers are normally formed within a week because of expansion and differentiation of muscle satellite cells (Chargé and Rudnicki, 2004). Satellite cells are a small population of myogenic stem cells for muscle regeneration, which are normally mitotically quiescent. After injury, satellite cells initiate proliferation to produce myogenic precursor cells, or myoblasts, to mediate the regeneration of muscle (Collins, 2006). The myoblasts undergo multiple rounds of cell division before terminal differentiation and formation of multinucleated myotubes by cell fusion.

During muscle development, somite-derived myoblasts differentiate into multinucleated skeletal muscle fibers. Myoblasts that fail to form muscle fibers initiate apoptosis and are rapidly lost (Asakura and Tapscott, 1998; Borycki et al., 1999; Kassar-Duchossoy et al., 2005; Relaix et al., 2005; Schwartz et al., 2009). The state of myogenic differentiation influences the propensity of myoblasts to undergo apoptosis (Walsh, 1997). The coordinated regulation of cell proliferation, differentiation, and apoptosis is necessary to control the deposition of muscle mass during myogenesis. Recent work demonstrates that the molecules regulating the apoptosis cascade, such as caspase-3 and caspase-8, are also involved in differentiation and syncytial fusion in both skeletal muscle fibers and placental villous trophoblast (Fidziańska and Goebel, 1991; Huppertz et al., 2001; Dee et al., 2002; Fernando et al., 2002). However, it remains to be elucidated how molecular events select terminal differentiation or apoptosis during myogenesis.

MyoD is a myogenic basic helix-loop-helix transcription factor that plays essential roles in satellite cell activation, proliferation, and differentiation (Sabourin et al., 1999; Cornelison et al., 2000; Asakura et al., 2007). Satellite cell–derived myoblasts isolated from adult mice lacking the *MyoD* gene (*MyoD*$^{-/-}$) display accelerated growth rates, delayed terminal differentiation, and delayed muscle regeneration (Megeney et al., 1996; Sabourin et al., 1999; Cornelison et al., 2000; White et al., 2000). Recently,

Correspondence to Atsushi Asakura: asakura@umn.edu

Abbreviations used in this paper: APC, allophycocyanin; ASC, activated satellite cell; ChIP, chromatin IP; CMV, cytomegalovirus; CTX, cardiotoxin; Cyt *c*, cytochrome *c*; IP, immunoprecipitation; KD, knockdown; Luc, luciferase; MHC, myosin heavy chain; miRNA, microRNA; PE, phycoerythrin; QSC, quiescent satellite cell; shRNA, short hairpin RNA; UTR, untranslated region.

© 2010 Hirai et al. This article is distributed under the terms of an Attribution–Noncommercial–Share Alike–No Mirror Sites license for the first six months after the publication date (see http://www.rupress.org/terms). After six months it is available under a Creative Commons License (Attribution–Noncommercial–Share Alike 3.0 Unported license, as described at http://creativecommons.org/licenses/by-nc-sa/3.0/).

The Rockefeller University Press $30.00
J. Cell Biol. Vol. 191 No. 2 347–365
www.jcb.org/cgi/doi/10.1083/jcb.201006025

THE JOURNAL OF CELL BIOLOGY

Downloaded from http://rupress.org/jcb/article-pdf/191/2/347/1869953/jcb_201006025.pdf by guest on 06 December 2025

we demonstrated that after injection into injured muscle, *MyoD*$^{-/-}$ myoblasts engrafted with significantly higher efficiency than wild-type myoblasts (Asakura et al., 2007). In addition, *MyoD*$^{-/-}$ myoblast–derived satellite cells were detected underneath the basal lamina of muscle fibers, indicating that *MyoD*$^{-/-}$ myoblasts are capable of self-renewal. Importantly, *MyoD*$^{-/-}$ myoblasts were revealed to possess remarkable resistance to apoptosis with increased survival compared with wild-type myoblasts. Therefore, *MyoD*$^{-/-}$ myoblasts may preserve stem cell characteristics including their resistance to apoptosis, efficiency of engraftment, and improvement in satellite cell contribution after transplantation. However, it remained unclear how MyoD actively regulates the apoptotic cascade in myoblasts. In this study, we demonstrate that MyoD not only regulates terminal differentiation but also apoptosis through microRNA (miRNA)-mediated down-regulation of Pax3.

Results

MyoD$^{-/-}$ myoblasts are resistant to apoptosis during muscle regeneration

Previously, we reported that *MyoD*$^{-/-}$ myoblasts display greater resistance to apoptosis under differentiation conditions and a significantly higher engraftment rate after intramuscular transplantation compared with wild-type myoblasts (Asakura et al., 2007). Therefore, we first examined the extent of apoptosis in skeletal muscle after cardiotoxin (CTX) injection, which induces muscle damage with successive muscle regeneration. Together, immunostaining for Pax7, a marker for satellite cells and myogenic precursor cells, and TUNEL staining clearly indicated that wild-type tibialis anterior (TA) muscle displays more apoptotic satellite cells and myogenic precursor cells than *MyoD*$^{-/-}$ muscle 2 d after CTX injection (Fig. 1, A and B). Next, we compared apoptosis levels after myoblast injection into regenerating TA muscle. Myoblasts were prepared from skeletal muscle of the control *Rosa26* and *MyoD*$^{-/-}$*:Rosa26* adult mice. 2 d after cell injection into regenerating TA muscle, double immunostaining for Pax7 and activated caspase-3 clearly indicated that more lacZ^{+} *Rosa26* myoblasts and their progenies underwent apoptosis compared with *MyoD*$^{-/-}$*:Rosa26* cells (Fig. 1, C and D).

MyoD is an activator for caspase-3 and apoptosis

Next, we examined whether MyoD-induced apoptosis was the result of caspase-3 activation. Caspase-3 activity and TUNEL staining clearly indicated that wild-type myoblasts showed higher caspase-3 activity and underwent more apoptosis in differentiation conditions compared with *MyoD*$^{-/-}$ myoblasts (Figs. 2 A and S2 A). In addition, UV exposure, a DNA damage inducer (Sabourin et al., 1999), and treatment with thapsigargin, an ER stress inducer (Morishima et al., 2004), led to higher caspase-3 activity in wild-type myoblasts compared with *MyoD*$^{-/-}$ myoblasts (Figs. 2 A and S2 A). Collectively, these data confirmed that *MyoD*$^{-/-}$ myoblasts display low caspase-3 activity and are resistant to apoptosis under both in vivo and in vitro conditions versus typical apoptotic characteristics observed in wild-type myoblasts.

Next, we examined whether MyoD expression could induce apoptosis. Infection with a lentivirus vector expressing MyoD effectively rescued MyoD protein expression in *MyoD*$^{-/-}$ myoblasts, detected by Western blotting and immunostaining (Fig. S2, B and C). More than 90% of *MyoD*$^{-/-}$ myoblasts became MyoD positive after infection. Ectopic expression of MyoD in *MyoD*$^{-/-}$ myoblasts resulted in induction of myosin heavy chain (MHC)–positive muscle differentiation, indicating that MyoD protein transduced by the lentivirus vector was functional (Fig. S2 C). Differentiation conditions, UV exposure, and thapsigargin treatment led to much higher caspase-3 activity (at day 4; 3.6-fold, 14.5-fold, and 9.0-fold, respectively) when MyoD was expressed in *MyoD*$^{-/-}$ myoblasts as compared with control *MyoD*$^{-/-}$ myoblasts (Fig. 2, B and C).

To examine whether acute loss of MyoD was sufficient to protect against apoptosis in wild-type myoblasts, we created MyoD knockdown (KD) myoblasts through infection with a lentivirus vector expressing short hairpin RNA (shRNA) for MyoD. MyoD KD wild-type myoblasts showed >80% reduction in MyoD protein expression compared with the control myoblasts, as judged by immunostaining and Western blotting (Fig. S2, D–F). Importantly, under differentiation condition or after UV exposure or thapsigargin treatment, cell death and caspase-3 activity were partially suppressed in MyoD KD myoblasts compared with the control myoblasts (Fig. 2, D and E). Collectively, the ectopic expression of MyoD and MyoD KD experiments strongly suggest that MyoD regulates the apoptosis cascade as a proapoptotic factor during muscle differentiation.

MyoD suppresses antiapoptotic genes Bcl-2, Bcl-xL, and Pax3

To reveal the molecular cascade of apoptosis regulated by MyoD, we examined antiapoptotic and proapoptotic gene expression (Kuwana and Newmeyer, 2003) in wild-type versus *MyoD*$^{-/-}$ myoblasts by semiquantitative RT-PCR and Western blotting. Among antiapoptotic Bcl-2 family genes, we noticed that *MyoD*$^{-/-}$ myoblasts markedly up-regulated gene and protein expression of Bcl-2 and Bcl-xL in control growth medium and after UV exposure and treatment with thapsigargin (Figs. 3 A, 4 A, and S3 A). In addition, some proapoptotic protein gene expression, such as Bim and Noxa, were slightly decreased in *MyoD*$^{-/-}$ myoblasts. Therefore, the altered antiapoptotic and proapoptotic protein expression may cause resistance to apoptosis in *MyoD*$^{-/-}$ myoblasts. It is well known that both Bcl-2 and Bcl-xL prevent the release of proteins such as cytochrome *c* (Cyt *c*), an activator for caspase protease, from the mitochondria (Kuwana and Newmeyer, 2003). We found that after UV exposure and treatment with thapsigargin, wild-type myoblasts induced the cytoplasmic translocation of Cyt *c* (Fig. 3 A). In contrast, *MyoD*$^{-/-}$ myoblasts failed to release Cyt *c*, whereas ectopic expression of MyoD in *MyoD*$^{-/-}$ myoblasts induced the cytoplasmic translocation of Cyt *c* (Fig. 3 B). In addition, MyoD KD in wild-type myoblasts decreased cytoplasmic translocation of Cyt *c* only under the strong apoptotic conditions (Fig. 3 C).

Recent studies demonstrate that Pax3 and Pax7 function as survival factors during embryonic and postnatal myogenesis (Borycki et al., 1999; Pani et al., 2002; Kassar-Duchossoy et al.,

Downloaded from http://rupress.org/jcb/article-pdf/191/2/347/1869953/jcb_201006025.pdf by guest on 06 December 2025

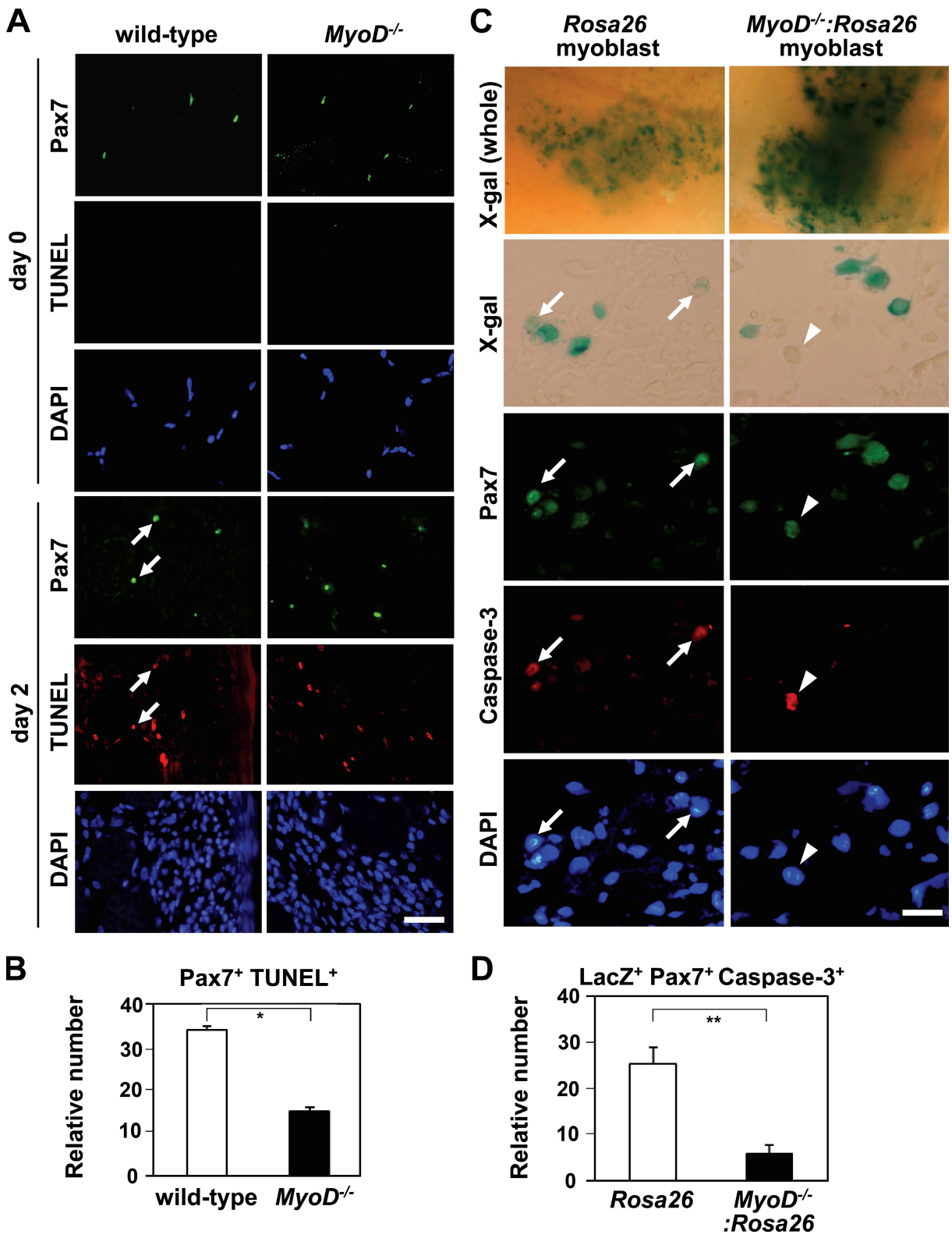

Figure 1. ***MyoD*$^{-/-}$ myogenic precursor cells are resistant to apoptosis in vivo.** (A) Before CTX injection (day 0), no Pax7$^+$ TUNEL$^+$ apoptotic satellite cells were detected in wild-type and *MyoD*$^{-/-}$ TA muscles. 2 d after CTX injection, Pax7$^+$ TUNEL$^+$ apoptotic myogenic precursor cells (arrows) were detected in wild-type muscles. Bar, 20 µm. (B) Number of Pax7$^+$ TUNEL$^+$ apoptotic myogenic precursor cells was quantified. (C) 1 d after CTX injection, myoblasts prepared from *Rosa26* or *MyoD*$^{-/-}$*:Rosa26* mice were intramuscularly injected into regenerating TA muscle. By 2 d after cell injection, lacZ$^+$ Pax7$^+$ donor-derived myogenic precursor cells were examined for activated caspase-3 expression (arrows). Arrowheads denote lacZ$^-$ Pax7$^+$ activated caspase-3$^+$ endogenous myogenic precursor cells. Bar, 10 µm. (D) The number of lacZ$^+$ Pax7$^+$ activated caspase-3$^+$ apoptotic myogenic precursor cells was measured. Nuclei were counterstained with DAPI (blue). *, $P < 0.05$; **, $P < 0.01$. Error bars indicate SEM.

Downloaded from http://rupress.org/jcb/article-pdf/191/2/347/1869953/jcb_201006025.pdf by guest on 06 December 2025

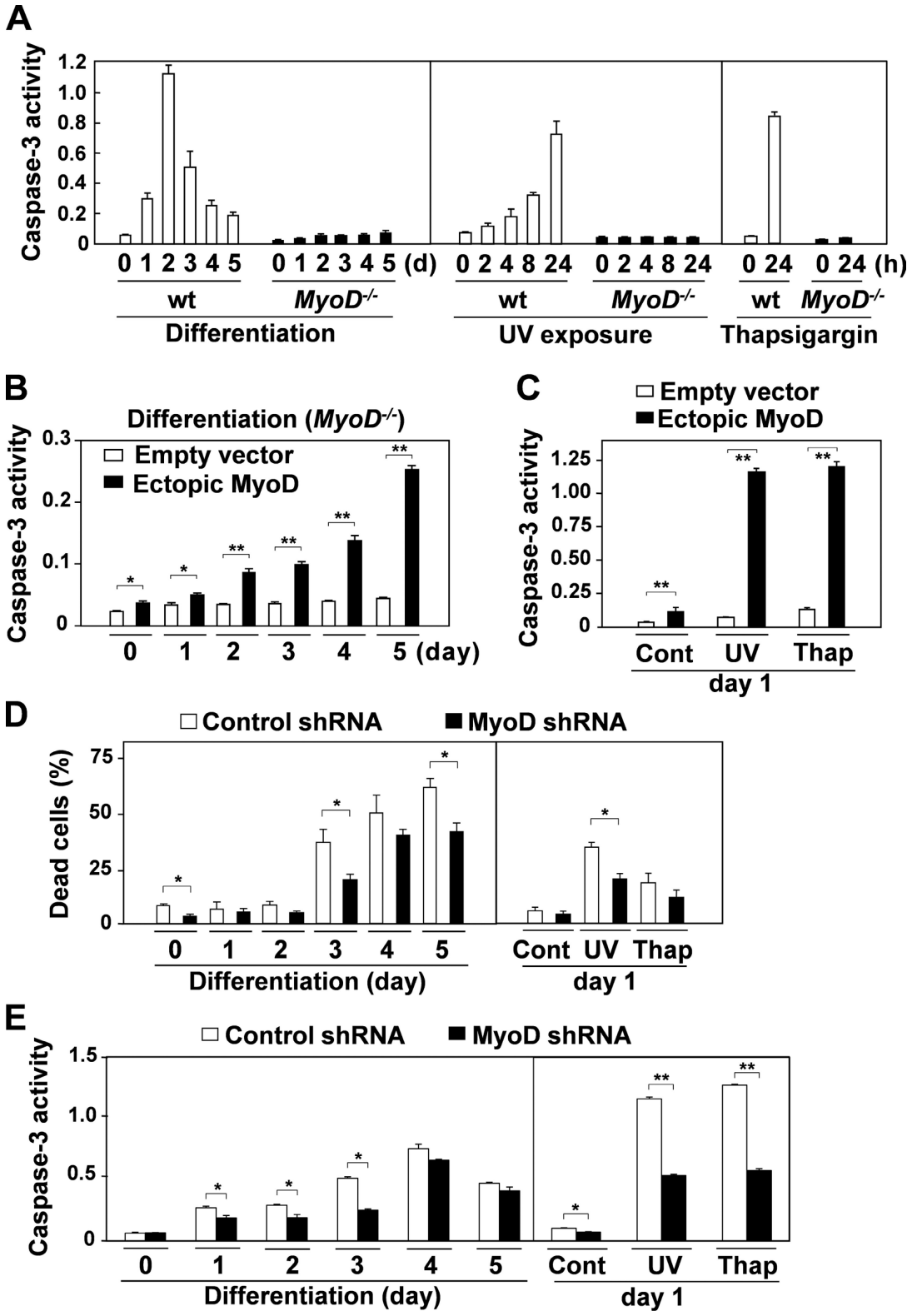

Figure 2. **Expression of MyoD induces apoptosis.** (A) Caspase-3 activity was compared between wild-type (wt) and *MyoD*$^{-/-}$ myoblasts under differentiation conditions from day 0 to 5 or UV exposure or treatment with thapsigargin from 0 to 24 h. (B) Under differentiation conditions from day 0 to 5, caspase-3 activity was compared between *MyoD*$^{-/-}$ myoblasts infected with a lentivirus vector expressing ectopic MyoD and a control empty vector. (C) After UV exposure or treatment with thapsigargin (Thap) for 1 d, caspase-3 activity was compared between *MyoD*$^{-/-}$ myoblasts infected with a lentivirus vector expressing ectopic MyoD and a control empty vector. (D and E) Under differentiation conditions from day 0 to 5 or after UV exposure or treatment with thapsigargin (Thap) for 1 d, cell death (D) and caspase-3 activity (E) were compared between wild-type myoblasts infected with a lentiviral vector expressing shRNA for MyoD and a control shRNA vector. *, $P < 0.05$; **, $P < 0.01$. Error bars indicate SEM.

Downloaded from http://rupress.org/jcb/article-pdf/191/2/347/1869953/jcb_201006025.pdf by guest on 06 December 2025

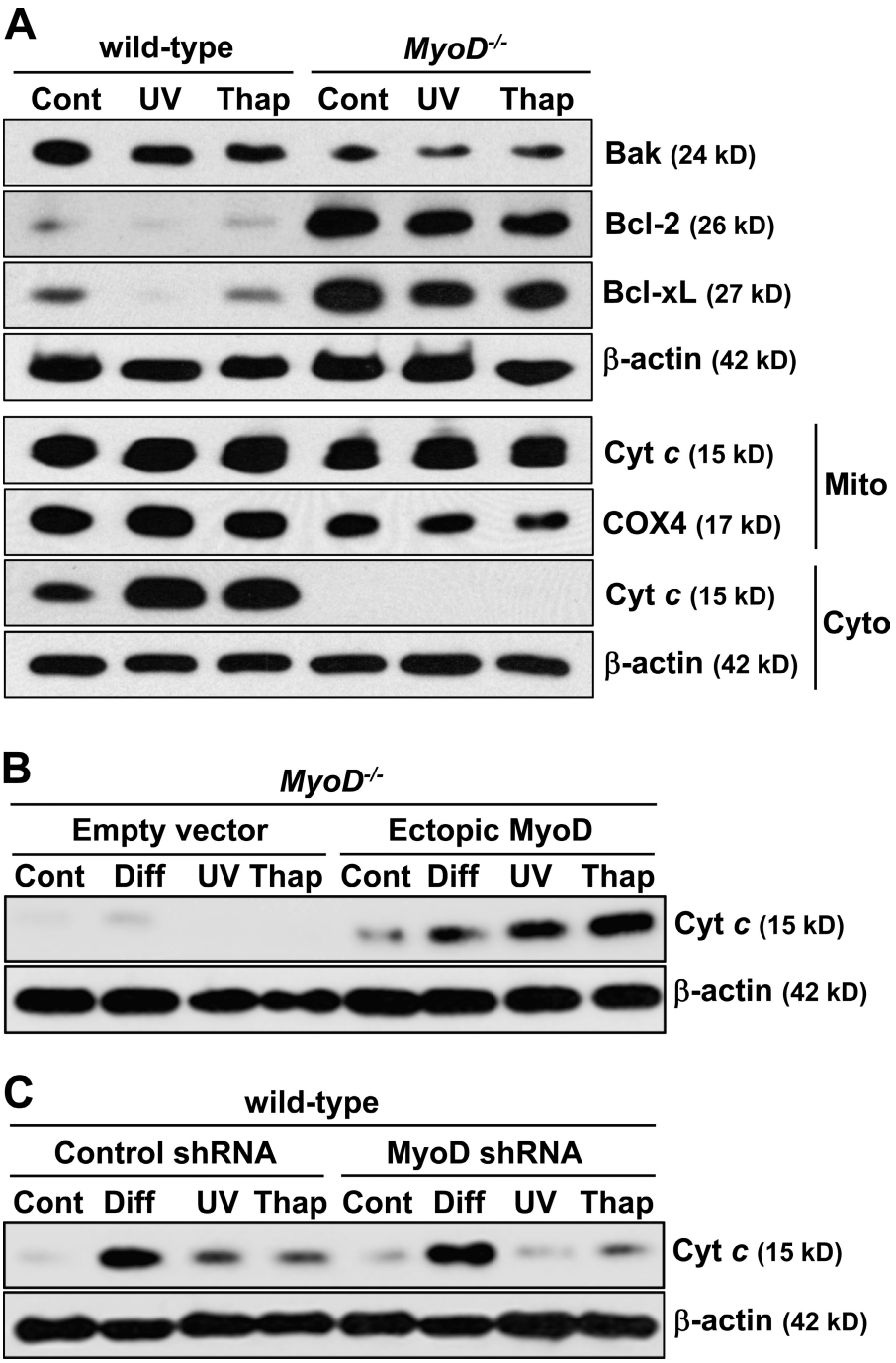

Figure 3. ***MyoD*$^{-/-}$ myoblasts up-regulate antiapoptotic proteins Bcl-2 and Bcl-xL and induce Cyt *c* release.** (A) Expression of antiapoptotic proteins Bcl-2 and Bcl-xL and proapoptotic protein Bak in wild-type and *MyoD*$^{-/-}$ myoblasts was assessed by Western blotting under growth conditions (control [Cont]) or after UV exposure or treatment with thapsigargin (Thap) for 1 d. Mitochondrial (Mito) and cytoplasmic (Cyto) protein extracts were also probed with antibodies against COX4, Cyt *c*, or β-actin. (B) Cyt *c* translocation into cytoplasm in *MyoD*$^{-/-}$ myoblasts was assessed by Western blotting after infection with a lentivirus vector expressing MyoD or a control empty vector under growth conditions, differentiation conditions (Diff) for 3 d, or after UV exposure or treatment with thapsigargin for 1 d. (C) Cyt *c* translocation into cytoplasm in wild-type myoblasts was assessed by Western blotting after infection with a lentivirus vector expressing shRNA for MyoD or a control shRNA vector under growth conditions, differentiation conditions for 3 d, or after UV exposure or treatment with thapsigargin for 1 d. β-Actin was monitored as a loading control.

2005; Relaix et al., 2006). Therefore, we compared their expression levels between wild-type and *MyoD*$^{-/-}$ myoblasts. Interestingly, Pax3 gene and protein expression were highly up-regulated in *MyoD*$^{-/-}$ myoblasts (8.3-fold in protein level) compared with wild-type myoblasts, in which Pax3 expression levels were very low or nondetectable, as reported previously (Fig. 4, A–D; Montarras et al., 2005). In contrast, Pax7 gene and protein expression were not altered between the two cell types (Fig. 4, A and B). Similar up-regulation of Pax3 protein (4.7-fold) was also detected in isolated hind limb muscle from *MyoD*$^{-/-}$ mice compared with wild-type mice (Fig. S4, A and B). Importantly, the ectopic expression of MyoD in *MyoD*$^{-/-}$ myoblasts down-regulated Pax3, Bcl-2, and Bcl-xL gene and protein expression (Fig. 5, A–C). In contrast, MyoD KD in wild-type myoblasts increased gene expression of Bcl-2 and Pax3 (Fig. 5 A) along with protein expression of Pax3, Bcl-2, and Bcl-xL (Fig. 5, B and C). However, altered MyoD expression level did not change Pax7 gene expression (Fig. 5 A). These results suggest that MyoD negatively regulates Bcl-2, Bcl-xL, and Pax3, which activate the apoptotic cascade.

A previous study demonstrated that Pax3 acts as a transcription factor for Bcl-xL gene expression by binding to the regulatory region of the Bcl-xL gene (Margue et al., 2000). Therefore, up-regulation of Pax3 in *MyoD*$^{-/-}$ myoblasts may

Downloaded from http://rupress.org/jcb/article-pdf/191/2/347/1869953/jcb_201006025.pdf by guest on 06 December 2025

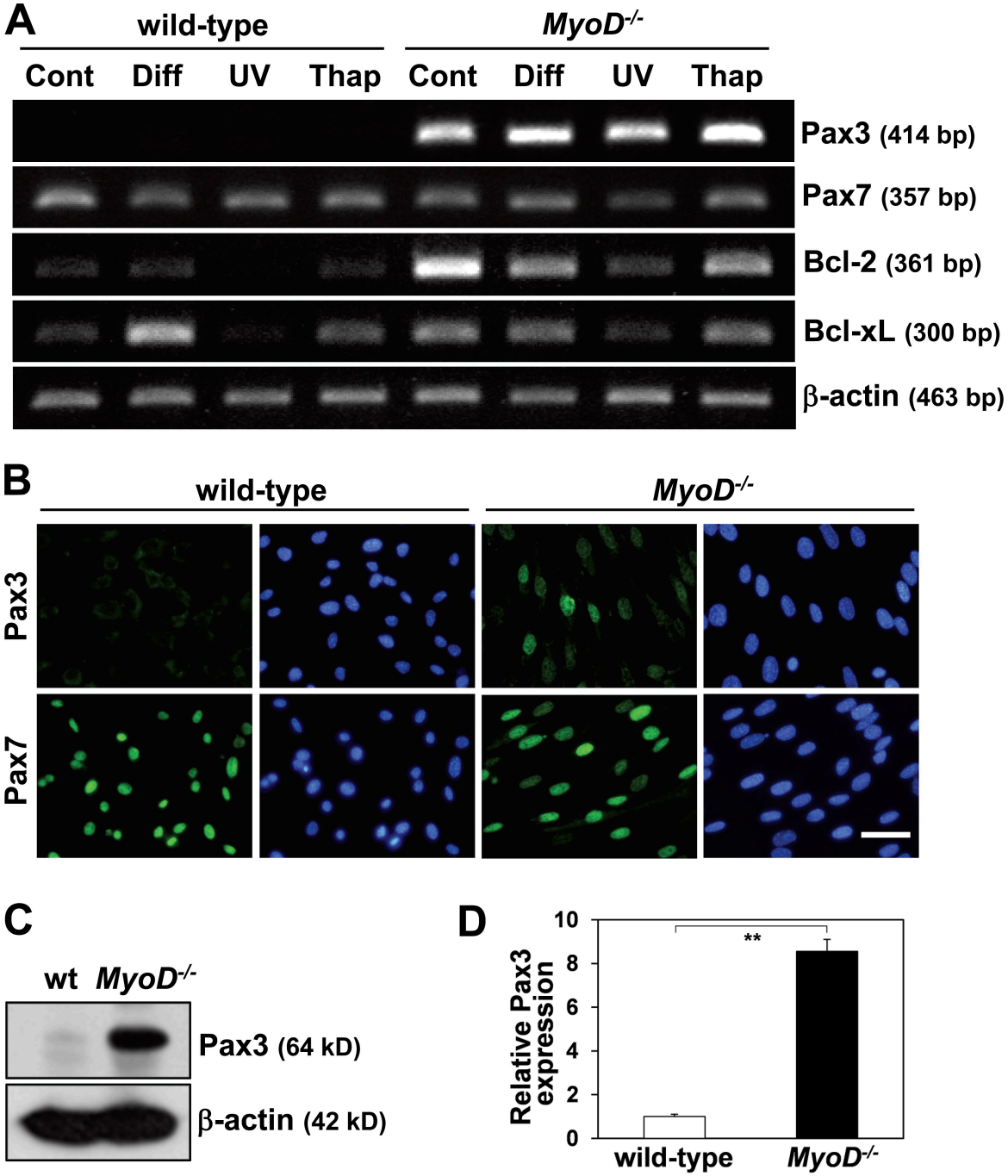

Figure 4. ***MyoD*$^{-/-}$ myoblasts up-regulate Pax3 expression.** (A) Under growth conditions (control [Cont]), differentiation conditions (Diff), UV exposure, or treatment with thapsigargin (Thap), Pax3, Pax7, Bcl-2, and Bcl-xL gene expression were compared between wild-type and *MyoD*$^{-/-}$ myoblasts by RT-PCR. (B) Pax3 and Pax7 expression were compared between wild-type and *MyoD*$^{-/-}$ myoblasts by immunostaining (green). Nuclei were counterstained with DAPI (blue). Bar, 40 µm. (C) Pax3 protein expression was compared between wild-type (wt) and *MyoD*$^{-/-}$ myoblasts by Western blotting. (D) Relative Pax3 expression levels normalized by β-actin expression shown in C were measured. (A and C) β-Actin was monitored as a loading control. **, $P < 0.01$. Error bars indicate SEM.

cause transcriptional up-regulation of Bcl-2 and Bcl-xL and, thus, myoblast resistance to apoptosis. Supporting this hypothesis, ectopic expression of Pax3 in wild-type myoblasts increased gene and protein expression of Bcl-2 (8.7-fold for protein) and Bcl-xL (4.0-fold for protein; Fig. 6, A–C). In contrast, Pax3 KD by siRNA in *MyoD*$^{-/-}$ myoblasts down-regulated gene and protein expression of Bcl-2 (5.5-fold for protein) and Bcl-xL (4.4-fold for protein; Fig. 6, A, B, and D).

To test whether Pax3 functioned as a transcriptional regulator for Bcl-2 and Bcl-xL genes, we performed luciferase (Luc) assays using the Bcl-2 and Bcl-xL promoters driving Luc reporter genes (Fig. 6 E). Activation of both Bcl-2– and Bcl-xL–Luc

Downloaded from http://rupress.org/jcb/article-pdf/191/2/347/1869953/jcb_201006025.pdf by guest on 06 December 2025

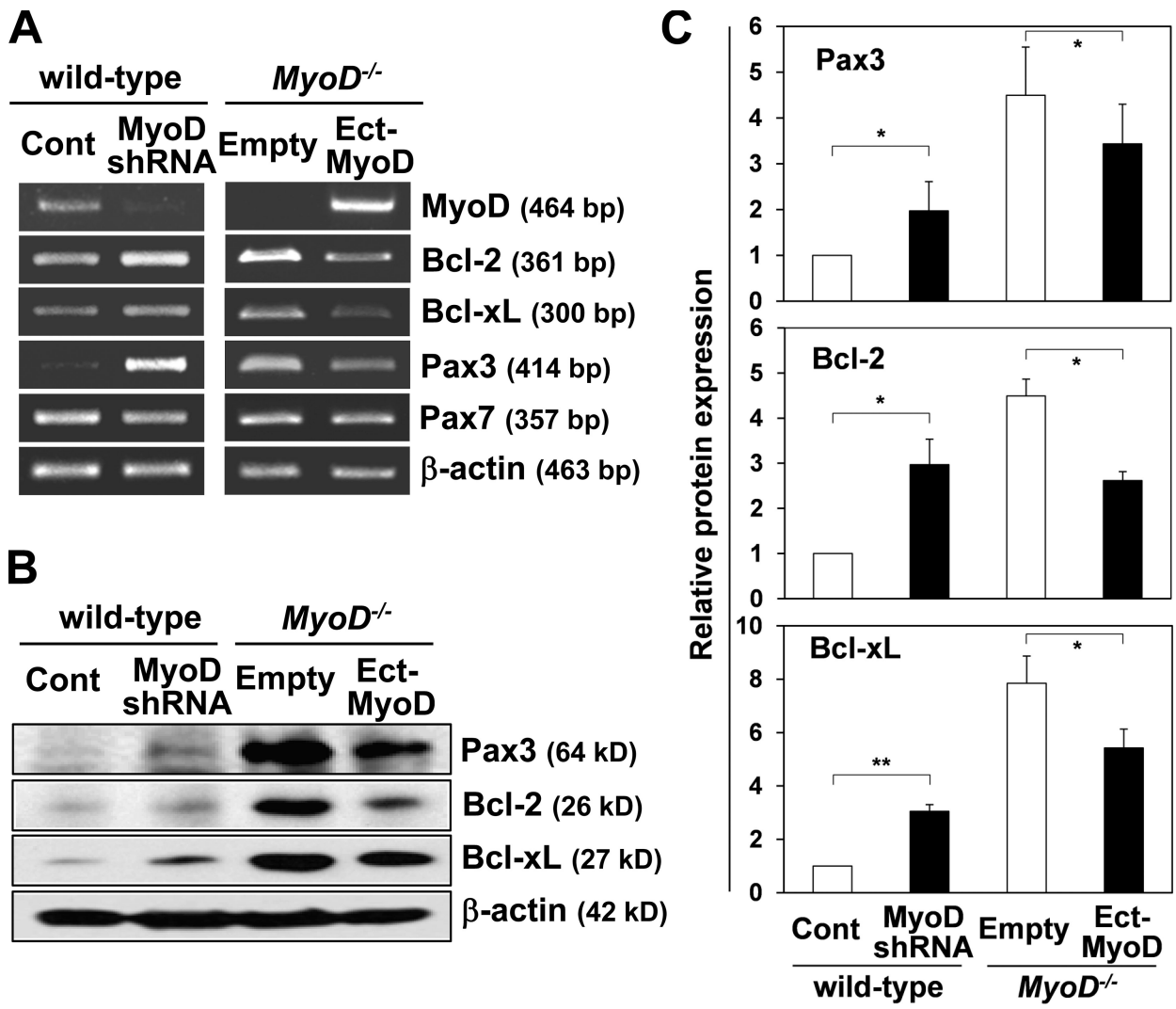

Figure 5. **MyoD negatively regulates Pax3, Bcl-2, and Bcl-xL expression.** (A) MyoD, Bcl-2, Bcl-xL, Pax3, and Pax7 gene expression were compared between wild-type myoblasts infected with a lentivirus vector expressing shRNA vector for MyoD and a control shRNA vector (Cont) or *MyoD*$^{-/-}$ myoblasts infected with a lentivirus vector expressing MyoD (Ect-MyoD) and a control empty vector by RT-PCR. (B) Bcl-2, Bcl-xL, and Pax3 protein expression were compared between wild-type myoblasts infected with a lentivirus vector expressing shRNA vector for MyoD and a control shRNA vector or *MyoD*$^{-/-}$ myoblasts infected with a lentivirus vector expressing MyoD and a control empty vector by Western blotting. (A and B) β-Actin was monitored as a loading control. (C) Relative Pax3, Bcl-2, and Bcl-xL protein expression levels normalized by β-actin expression were measured by Western blotting. *, $P < 0.05$; **, $P < 0.01$. Error bars indicate SEM.

reporter genes was higher in *MyoD*$^{-/-}$ myoblasts compared with wild-type myoblasts (1.8-fold and 1.7-fold, respectively). Ectopic expression of Pax3 activated both Bcl-2– and Bcl-xL–Luc reporter genes in wild-type myoblasts (4.0-fold and 2.3-fold, respectively), strongly suggesting that Pax3 is a transcriptional activator for Bcl-2 and Bcl-xL genes. Consequently, ectopic expression of Pax3 displayed decreased cell death under the differentiation conditions (2.0-fold at day 2) and after UV exposure (2.5-fold) and treatment with thapsigargin (1.8-fold; Fig. 6 F). Finally, after UV exposure, ectopic expression of Pax3 reduced caspase-3 activity in wild-type myoblasts (3.1-fold), whereas Pax3 KD increased caspase-3 activity in *MyoD*$^{-/-}$ myoblasts (2.3-fold; Fig. 6 G), indicating the antiapoptotic role for Pax3. Collectively, these results indicate that MyoD deficiency increases Pax3, enhancing Bcl-2 and Bcl-xL gene expression to provide resistance to apoptosis in *MyoD*$^{-/-}$ myoblasts. Therefore, we concluded that MyoD negatively regulates Pax3 expression in myoblasts by transcriptional and/or posttranscriptional regulation.

MyoD suppresses Pax3 through activation of miRNA, miR-1, and miR-206

Recent work demonstrates that MyoD directly regulates the transcription of miRNA expression, which suppresses specific targets during myogenic differentiation by blocking protein translation and/or by RNA degradation (Chen et al., 2006). We identified two potential miR-1– and miR-206–binding sites within the 3′ untranslated region (UTR) of Pax3 mRNA (Fig. 7 A). Both miR-1 and miR-206 are known MyoD-targeting miRNAs (Rao et al., 2006). We termed these two potential miR-1– and miR-206–binding sites M1 and M2, respectively. Both core sequences are highly conserved among vertebrates, suggesting

Downloaded from http://rupress.org/jcb/article-pdf/191/2/347/1869953/jcb_201006025.pdf by guest on 06 December 2025

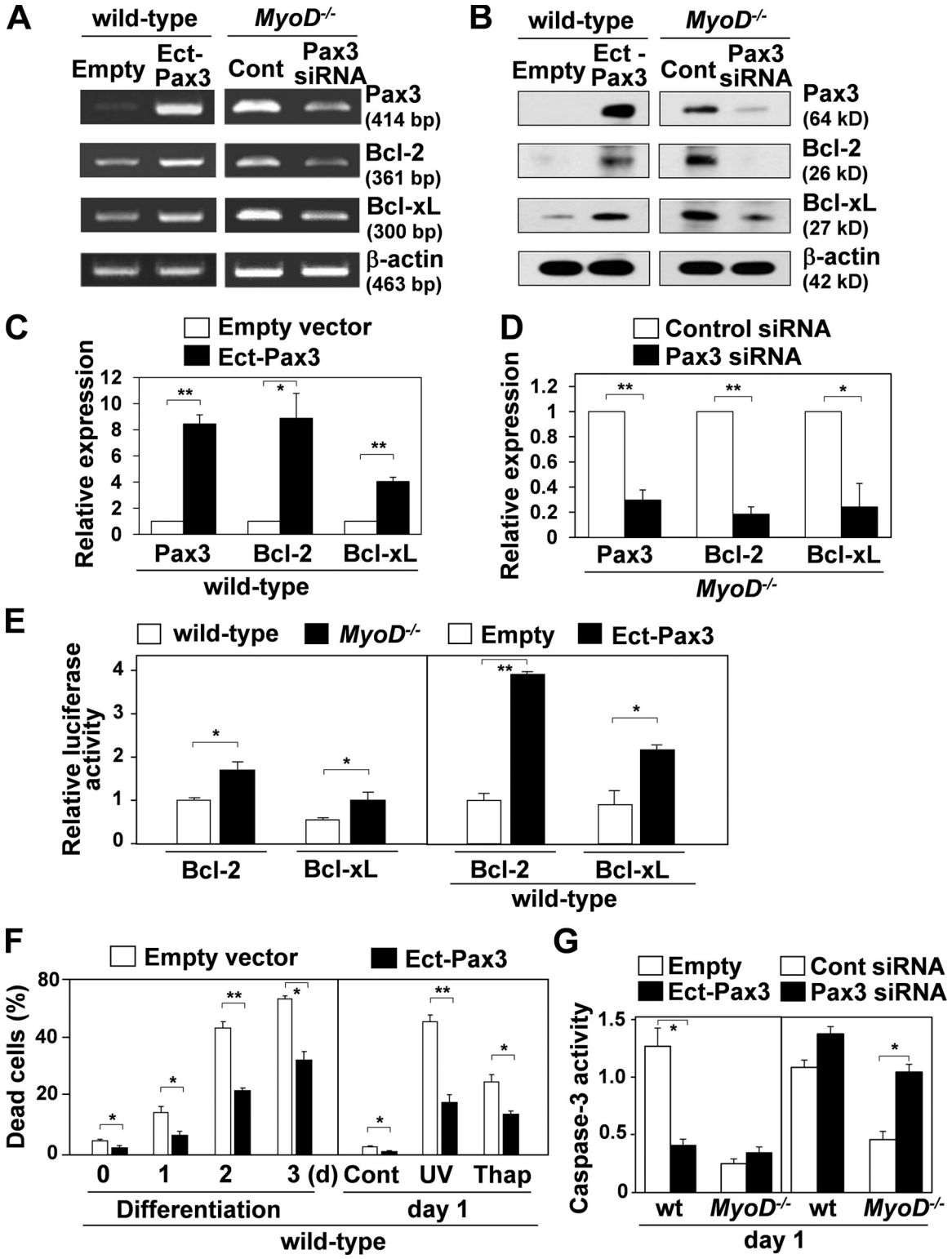

Figure 6. **Pax3 positively regulates Bcl-2 and Bcl-xL expression.** (A) Pax3, Bcl-2, and Bcl-xL gene expression were compared between wild-type myoblasts infected with a retrovirus vector expressing Pax3 (Ect-Pax3) and a control empty vector or *MyoD*$^{-/-}$ myoblasts transfected with siRNA for Pax3 and a control siRNA (Cont) by RT-PCR. (B) Pax3, Bcl-2, and Bcl-xL protein expression were compared between wild-type myoblasts infected with a retrovirus vector expressing Pax3 and a control empty vector or *MyoD*$^{-/-}$ myoblasts transfected with siRNA for Pax3 and a control siRNA by Western blotting. (A and B) β-Actin was monitored as a loading control. (C and D) Relative Pax3, Bcl-2, and Bcl-xL protein expression levels shown in B normalized by β-actin expression were compared by Western blotting. (E) Luc activity was assessed after transfection with Bcl-2– or Bcl-xL–Luc reporter genes into wild-type or *MyoD*$^{-/-}$ myoblasts. Luc activity was also assessed after transfection with Bcl-2– or Bcl-xL–Luc reporter genes and the Pax3 expression vector or control empty vector into wild-type myoblasts. (F) Under differentiation conditions from day 0 to 3 or after UV exposure or treatment with thapsigargin (Thap) for 1 d, cell death was compared between wild-type myoblasts infected with a retrovirus vector expressing Pax3 and a control empty vector. (G) After UV exposure or treatment with thapsigargin for 1 d, caspase-3 activity was compared between wild-type and *MyoD*$^{-/-}$ myoblasts infected with a retrovirus vector expressing Pax3 and a control empty vector or transfected with siRNA for Pax3 and a control siRNA. *, $P < 0.05$; **, $P < 0.01$. Error bars indicate SEM.

Downloaded from http://rupress.org/jcb/article-pdf/191/2/347/1869953/jcb_201006025.pdf by guest on 06 December 2025

the importance of these sites for Pax3 regulation (Fig. 7, A and B). For mouse Pax3, there are two putative polyA signal sequences in the 3′UTR. Both proximal (polyA1) and distal (polyA2) polyA signal sequences were indeed used for transcription of Pax3 mRNAs with the shorter and longer 3′UTRs, respectively (Fig. 7 A). The longer 3′UTR contains both putative miR-1– and miR-206–binding sites. In contrast, the human Pax3 gene only contains polyA2 sequence, and thus, the human Pax3 mRNA contains the longer 3′UTR with the two putative miR-1/miR-206–binding sites (Barber et al., 1999). In both human and mouse Pax3 genes, there are several alternative splicing variants using multiple stop codons (Fig. 7 A). Semiquantitative RT-PCR data clearly showed that the longer 3′UTR was used for Pax3 expression in *MyoD*$^{-/-}$ myoblasts (Fig. 7 C), suggesting that miR-1/miR-206 may negatively regulate Pax3 expression through binding to M1 and/or M2 sites.

MyoD regulates transcription of several target miRNAs, including miR-1, miR-22, miR-100, miR-133a, miR-191, and miR-206 (Chen et al., 2006; Kim et al., 2006; Rao et al., 2006; Rosenberg et al., 2006). Among them, only miR-1 and miR-206 were markedly down-regulated in *MyoD*$^{-/-}$ myoblasts. Expression of miR-133a was also slightly down-regulated in MyoD$^{-/-}$ myoblasts. These data indicate that miR-1, miR-206, and miR-133a are direct downstream target genes of MyoD in primary myoblasts (Fig. 7 D). Recent work showed that miR-27b binds to the shorter 3′UTR to suppress Pax3 expression during embryonic myogenesis and satellite cell activation (Crist et al., 2009). However, expression of miR-27b was very low in both wild-type and *MyoD*$^{-/-}$ myoblasts. Therefore, MyoD-mediated Pax3 down-regulation is most likely to be mediated by miR-1 and miR-206 in primary myoblasts. Indeed, miR-1 and miR-206 were up-regulated in wild-type and *MyoD*$^{-/-}$ myoblasts by ectopic expression of MyoD (Fig. 7 E). In contrast, MyoD KD decreased both miRNAs in wild-type myoblasts. Expression of miR-1 or miR-206 indeed suppressed Pax3, Bcl-2, and Bcl-xL gene expression without affecting Pax7 gene expression (Fig. 7 F).

Next, we examined whether transfection of wild-type myoblasts with anti-miRNAs (antagomirs) directed against miR-1 and miR-206 promoted the expression of Pax3, Bcl-2, and Bcl-xL (Fig. 7 G). Clearly, transfection with antagomirs for miR-1 and miR-206 increased expression levels of Pax3, Bcl-2, and Bcl-xL compared with the control. The combination of antagomirs for miR-1 and miR-206 more efficiently up-regulated expression of Pax3, Bcl-2, and Bcl-xL without affecting Pax7 gene expression. It has been reported that Bcl-2 gene expression is suppressed by miR-15a and miR-16 (Cimmino et al., 2005). However, alteration of MyoD expression in wild-type or *MyoD*$^{-/-}$ myoblasts did not affect expression of these two miRNAs (Fig. S3 B), indicating that MyoD does not negatively regulate the transcription of Bcl-2 by means of these miRNAs.

To elucidate whether miR-1 and miR-206 directly bound to the 3′UTR of Pax3, we created Luc reporter genes conjugated with the longer Pax3-3′UTR (cytomegalovirus [CMV]-Luc-3′UTR) and the longer Pax3-3′UTR with mutations at M1 and M2 (CMV-Luc-3′UTRM; Fig. 8 A). As a result, MyoD transfection suppressed Luc activity in the wild-type reporter gene (CMV-Luc-3′UTR) but did not suppress Luc activity in the mutant reporter gene (CMV-Luc-3′UTRM) for both wild-type and *MyoD*$^{-/-}$ myoblasts (Fig. 8 B). Similarly, transfection of pre–miR-1 and pre–miR-206 also suppressed Luc activity in CMV-Luc-3′UTR in both wild-type (2.4-fold and 1.9-fold, respectively) and *MyoD*$^{-/-}$ myoblasts (2.8-fold and 2.0-fold, respectively) but did not suppress Luc activity in CMV-Luc-3′UTRM (Fig. 8 C). These results suggest the direct binding of miR-1/miR-206 to the M1 and/or M2 sites within the longer 3′UTR of Pax3. Importantly, transfection with pre–miR-1 and pre–miR-206 increased cell death in *MyoD*$^{-/-}$ myoblasts under differentiation conditions (3.0-fold and 3.1-fold at day 2 differentiation, respectively) and after UV exposure (2.7-fold and 2.8-fold, respectively) and treatment with thapsigargin (5.3-fold and 5.2-fold, respectively; Fig. 8 D). In addition, transfection of pre–miR-1 and pre–miR-206 increased MHC-positive myogenic differentiation of wild-type myoblasts, whereas overexpression of Pax3 partially suppressed myogenic differentiation (Fig. S4, C–E). Finally, transfection with antagomirs for miR-1 and miR-206 partially suppressed apoptosis after UV exposure and treatment with thapsigargin in both wild-type myoblasts and *MyoD*$^{-/-}$ myoblasts expressing ectopic MyoD (Fig. 8 E). These results strongly suggest that MyoD regulates the transcription of miR-1/miR-206 expression, which in turn directly suppresses Pax3 expression in myoblasts. Down-regulation of Pax3 results in down-regulation of Bcl-2 and Bcl-xL to induce apoptosis under stressful conditions.

To examine whether 3′UTR of Pax3 was important for the expression level of Pax3, we created retrovirus Pax3 expression vectors: one containing 3′UTR (Pax3-3′UTR) and another 3′UTR with mutations at M1 and M2 (Pax3-3′UTRM). Compared with Pax3 expression vector, Pax3-3′UTR expression vector showed significantly reduced Pax3 expression levels (2.6-fold) detected by immunostaining and RT-PCR (Fig. 9, A–C). This reduction was attenuated by mutations at M1 and M2 in the 3′UTR (Pax3-3′UTRM), confirming that Pax3-3′UTR is a target for miRNAs. These Pax3 expression levels affected caspase-3 activity in the myoblasts after treatment with thapsigargin. Although expression of Pax3 or Pax3-3′UTRM inhibited caspase-3 activity in wild-type myoblasts, this inhibition was reduced by Pax3-3′UTR expression (Fig. 9 D), suggesting that Pax3 expression levels regulated by the 3′UTR affect apoptosis in myoblasts.

Recently, *dicer* gene has been shown to process miRNA precursors into functional 21–23 nucleotide RNAs (Wang and Olson, 2009). *Dicer* gene knockout mice display early embryonic lethality with a variety of developmental phenotypes because of significant reduction in maturation of miRNAs (Harfe et al., 2005). We isolated satellite cell–derived myoblasts from *floxed dicer* adult mice (*dicer*$^{fl/fl}$). An adenovirus vector expressing a fusion gene of Cre recombinase and EGFP was infected to the *dicer*$^{fl/fl}$ myoblasts. 2 d after infection, most of the cells became EGFP^{+} and deleted *dicer* gene (Fig. 9, E and F). These myoblasts with deleted *dicer* gene display growth retardation and reduction of expression for several miRNAs and muscle-specific genes (Fig. 9 G). In contrast, expression of Pax3 was up-regulated in the myoblasts with deleted *dicer* gene, confirming that Pax3 gene expression is regulated by miRNAs.

Downloaded from http://rupress.org/jcb/article-pdf/191/2/347/1869953/jcb_201006025.pdf by guest on 06 December 2025

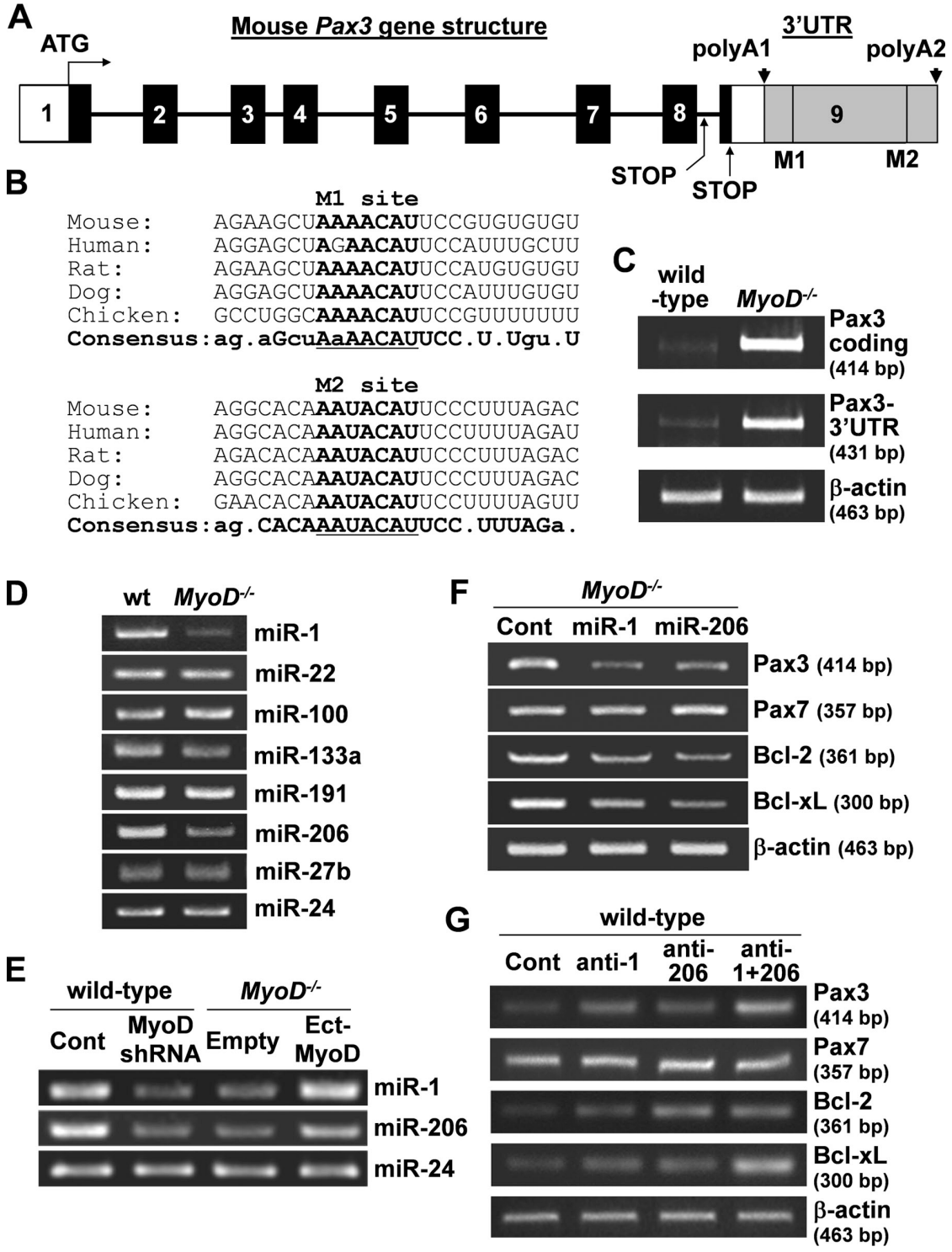

Figure 7. **Pax3-3′UTR contains conserved miR-1/miR-206–binding sites.** (A) Mouse Pax3 gene structure. Numbered boxes denote each exon. White boxes denote the 5′UTR and the shorter 3′UTR. Black boxes denote coding regions. The gray box denotes the longer 3′UTR containing two putative miR-1/miR-206–binding sites (M1 and M2). There are two stop codons and two polyA signal sequences (polyA1 and polyA2) in the mouse Pax3 gene. (B) Sequences of two putative miR-1/miR-206–binding sites (M1 and M2) and their flanking regions. Core sequences for miR-1/miR-206 and consensus sequences are denoted by bold letters. (C) Similar levels of expression of the Pax3 coding region and the longer 3′UTR were detected in *MyoD*$^{-/-}$ myoblasts by RT-PCR. β-Actin was monitored as a loading control. (D) MyoD-regulated miRNA expression levels were compared between wild-type (wt) and *MyoD*$^{-/-}$ myoblasts by RT-PCR. miR-24 was monitored as a loading control. (E) miR-1 and -206 expression were compared between wild-type myoblasts infected with a lentivirus vector expressing shRNA for MyoD and control shRNA (Cont) vector or *MyoD*$^{-/-}$ myoblasts infected with a lentivirus vector expressing MyoD (Ect-MyoD) and a control empty vector by RT-PCR. miR-24 was monitored as a loading control. (F) Pax3, Pax7, Bcl-2, and Bcl-xL gene expression were compared between *MyoD*$^{-/-}$ myoblasts transfected with pre–miR-1, pre–miR-206, and the control pre-miRNA by RT-PCR. β-Actin was monitored as a loading control. (G) Pax3, Pax7, Bcl-2, and Bcl-xL gene expression were compared between wild-type myoblasts transfected with anti–miR-1 (anti-1), anti–miR-206 (anti-206), anti–miR-1 + anti–miR-206 (anti-1 + 206), and the control RNA by RT-PCR. β-Actin was monitored as a loading control. (D and E) All PCR products are ∼90-bp long.

Downloaded from http://rupress.org/jcb/article-pdf/191/2/347/1869953/jcb_201006025.pdf by guest on 06 December 2025

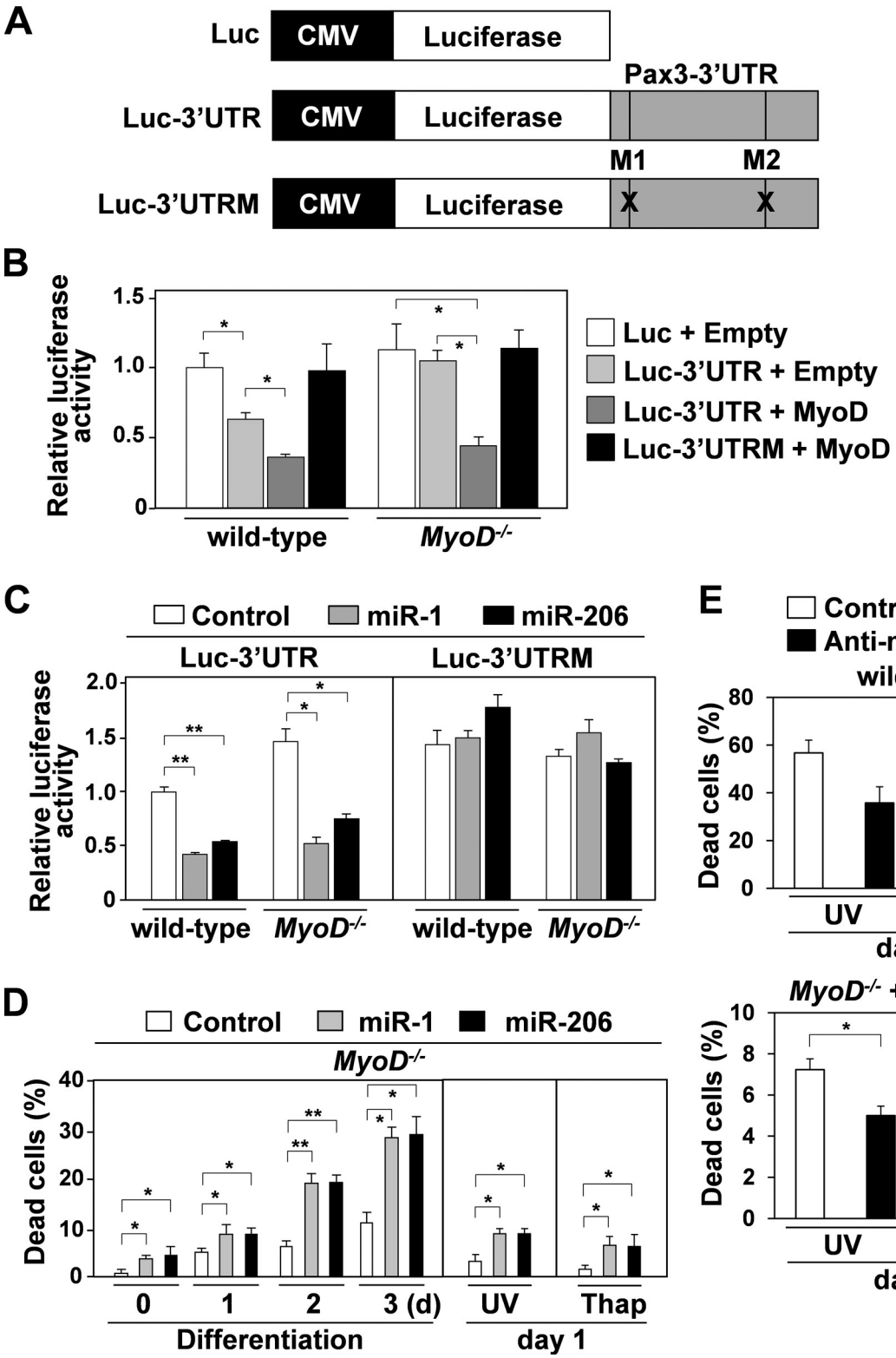

Figure 8. **Pax3-3′UTR is a target for miR-1 and miR-206.** (A) CMV promoter driving Luc reporter gene was used for creating Luc-3′UTR, which contains the longer Pax3-3′UTR fragment downstream of the Luc reporter gene. Two putative miR-1/miR-206–binding sites (M1 and M2) were mutated in Luc-3′UTRM. (B) Relative Luc activity was measured in wild-type and *MyoD*$^{-/-}$ myoblasts after transfection with control Luc reporter gene + empty expression vector, Luc-3′UTR + empty expression vector, Luc-3′UTR + MyoD expression vector, and Luc-3′UTRM + MyoD expression vector. (C) Relative Luc activity was measured in wild-type and *MyoD*$^{-/-}$ myoblasts after transfection with Luc-3′UTR + control pre-miRNA, Luc-3′UTR + pre–miR-1, Luc-3′UTR + pre–miR-206, Luc-3′UTRM + control pre-miRNA, Luc-3′UTRM + pre–miR-1, and Luc-3′UTRM + pre–miR-206. (D) Under differentiation conditions from day 0 to 3 or after UV exposure or treatment with thapsigargin (Thap) for 1 d, cell death was compared between wild-type myoblasts transfected with the control pre-miRNA, pre–miR-1, and pre–miR-206. (E) After UV exposure or treatment with thapsigargin for 1 d, cell death was compared between wild-type myoblasts or *MyoD*$^{-/-}$ myoblasts expressing ectopic MyoD transfected with the control miRNA or anti–miR-1 + anti–miR-206. *, $P < 0.05$; **, $P < 0.01$. Error bars indicate SEM.

Downloaded from http://rupress.org/jcb/article-pdf/191/2/347/1869953/jcb_201006025.pdf by guest on 06 December 2025

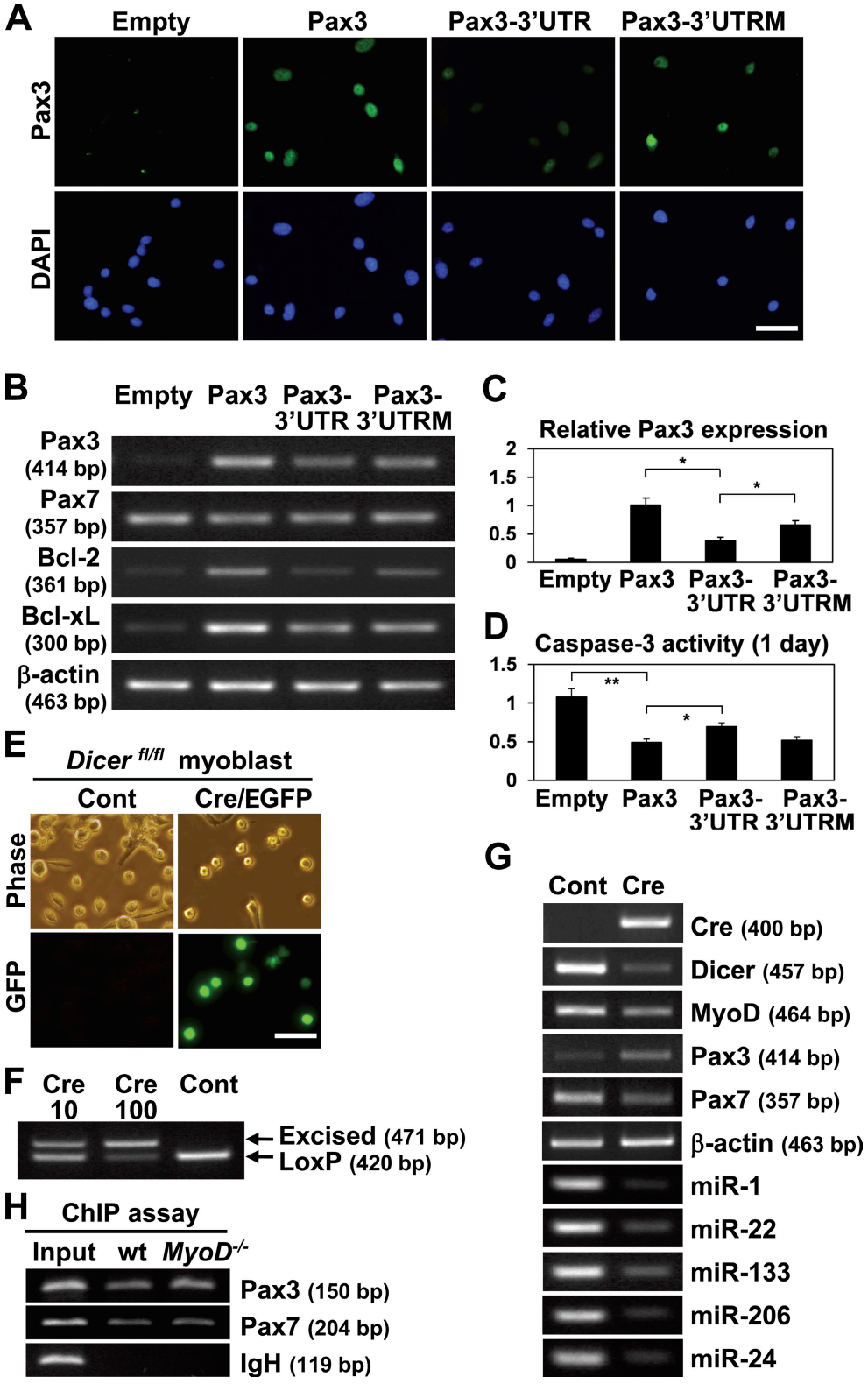

Figure 9. **Pax3 expression is regulated by dicer and Pax3-3′UTR.** (A) Pax3 expression was compared between wild-type myoblasts infected with a retrovirus vector expressing Pax3, Pax3-3′UTR, Pax3-3′UTR with mutations at miR-1/miR-206–binding sites (Pax3-3′UTRM), and a control empty vector by immunostaining (green). Nuclei were counterstained with DAPI (blue). (B) Pax3, Pax7, Bcl-2, and Bcl-xL gene expression were compared between wild-type myoblasts transfected with Pax3, Pax3-3′UTR, Pax3-3′UTRM, and a control empty vector by RT-PCR. (C) Relative Pax3 expression levels shown in B normalized by β-actin expression were measured. (D) After treatment with thapsigargin for 1 d, caspase-3 activity was compared between wild-type myoblasts infected with a retrovirus vector expressing Pax3, Pax3-3′UTR and Pax3-3′UTRM, and a control empty vector. (E) Myoblasts isolated from *floxed dicer* (*dicer*$^{fl/fl}$) mice were infected with adenovirus lacZ expression vector (control [Cont]) or adenovirus Cre/EGFP expression vector. GFP is only detected in myoblasts infected with adenovirus Cre/EGFP expression vector. (F) Control myoblasts infected with adenovirus lacZ expression vector shows the loxP band but not excised band after PCR. Infection with more adenovirus Cre/EGFP expression vector (10 and 100 µl) increased in amount of the excised band

Downloaded from http://rupress.org/jcb/article-pdf/191/2/347/1869953/jcb_201006025.pdf by guest on 06 December 2025

We have shown that expression of both Pax3 RNA and protein is considerably enhanced in MyoD-deficient myoblasts. It is not clear whether the augmentation of Pax3 RNA levels in these cells was caused by increased transcription or increased stability of the mRNA. Therefore, to examine whether there was differential transcription of the Pax3 gene in wild-type versus *MyoD*$^{-/-}$ myoblasts, a chromatin immunoprecipitation (IP [ChIP]) assay with antibodies against RNA polymerase II was performed (Fig. 9 H). Clearly, transcription of the Pax3 gene was still active in wild-type myoblasts, whereas it was relatively more active in *MyoD*$^{-/-}$ myoblasts. Therefore, Pax3 RNA level in wild-type myoblasts is regulated by transcriptional level and stability of the mRNA through miRNAs.

Recent work demonstrates that freshly isolated quiescent satellite cells (QSCs) display unique gene expression profiles (Fukada et al., 2007). In particular, QSCs do not express MyoD but, after isolation, become activated to activated satellite cells (ASCs) and up-regulate MyoD within 1 d (Cornelison et al., 2000; Zammit et al., 2002). In addition, some QSCs isolated from mouse hind limb down-regulate Pax3 gene and protein expression when they become ASCs (Montarras et al., 2005; Boutet et al., 2007; Crist et al., 2009). We isolated QSCs by FACS as CD45$^-$ CD31$^-$ Sca-1$^-$ integrin-α7$^+$ integrin-β1$^+$ fraction from hind limb muscles of wild-type and *MyoD*$^{-/-}$ mice. The percentages of integrin-α7 and -β1 double-positive QSCs per total events were slightly higher in *MyoD*$^{-/-}$ muscle (0.78 ± 0.01; $n = 3$) compared with wild-type muscle (0.70 ± 0.02; $n = 3$; Fig. S5 A), which is consistent with previously reported results (Megeney et al., 1996).

After sorting, QSCs were cultured to obtain ASCs. Semiquantitative RT-PCR confirmed that MyoD was absent in QSCs but present in wild-type ASCs at day 1 (Fig. 10 A). miR-1 and miR-206 were gradually up-regulated in wild-type ASCs with the highest levels at day 4, suggesting potential roles for miR-1 and miR-206 in satellite cell activation. Neither miR-1 nor miR-206 was detected in *MyoD*$^{-/-}$ QSCs or ASCs. Pax3, Bcl-2, and Bcl-xL were initially expressed in wild-type QSCs but quickly down-regulated in wild-type ASCs (Fig. 10, A and B). In *MyoD*$^{-/-}$ cells, Pax3, Bcl-2, and Bcl-xL expression were also high in QSCs but down-regulated in ASCs at days 1 and 2. In contrast to wild-type myoblasts, Pax3, Bcl-2, and Bcl-xL expression were retained in *MyoD*$^{-/-}$ ASCs at day 4 (Fig. 10, A and B).

Immunostaining clearly showed that most of the freshly isolated QSCs from both wild-type and *MyoD*$^{-/-}$ mice were positive for c-met, a marker for satellite cells (Fig. S5, B and C). Pax3-positive *MyoD*$^{-/-}$ QSCs (70.1%) were significantly higher than wild-type QSCs (30.1%). After culture, Pax3 expression was quickly down-regulated in Pax7-positive wild-type ASCs, as previously reported (Montarras et al., 2005; Boutet et al., 2007). In *MyoD*$^{-/-}$ ASCs, Pax3 was also down-regulated at day 1 (33.3% of cells) but still significantly higher than in wild-type ASCs (11.7% of cells). The ectopic expression of MyoD in *MyoD*$^{-/-}$ satellite cells down-regulated Pax3 gene expression. In contrast, MyoD KD in wild-type myoblasts increased gene expression of Pax3 (Fig. 10, C and D). Therefore, these results suggest that part of down-regulation of Pax3 may be mediated by MyoD-induced miR-1 and miR-206 during wild-type satellite cell activation. Collectively, these results suggest that MyoD can induce apoptosis through activation of miR-1 and miR-206 that decrease the level of the antiapoptotic protein Pax3, which in turn decreases Bcl-2 and Bcl-xL (Fig. 10 E).

Discussion

MyoD is a master transcription factor for myogenic specification and terminal differentiation (Weintraub et al., 1991). In this study, we demonstrate that MyoD not only regulates myogenic terminal differentiation but also acts as a proapoptotic factor. We have identified molecules downstream of MyoD that regulate apoptosis in myoblasts; negative regulation of Pax3 expression occurs through direct transcriptional activation of miR-1 and miR-206 gene expression. Pax3 is a survival factor that transcriptionally activates the antiapoptotic genes Bcl-2 and Bcl-xL. Therefore, negative regulation of Pax3 expression by MyoD-regulated miRNAs is a critical point for MyoD-dependent apoptosis in myoblasts.

One interesting notion is that skeletal muscle fibers and placental villous trophoblast are the main representatives of syncytia, which are derived from the fusion of mononucleated stem cells. The molecules regulating the apoptosis cascade, such as caspase-3 and caspase-8, are also involved in differentiation and syncytial fusion in both tissues (Huppertz et al., 2001; Fernando et al., 2002). Several studies have suggested that myogenic differentiation is accompanied by apoptosis (Sandri and Carraro, 1999). For example, proliferating C2C12 myoblasts can undergo either terminal differentiation or apoptosis under conditions of mitogen deprivation (Wang and Walsh, 1996). Previous work suggested a proapoptotic role for MyoD, showing that MyoD can promote apoptotic cell death in myoblasts when pRb function is lacking (Fimia et al., 1998; Peschiaroli et al., 2002). Recently, we and other groups have reported that MyoD deficiency led to the down-regulation of many antiapoptotic genes such as Bcl-2 (Asakura et al., 2007) and proapoptotic genes such as PUMA (Harford et al., 2010). Bcl-2 expression in myoblasts inhibits apoptosis and promotes clonal expansion (Dominov et al., 2005). Indeed, satellite cells from young rats had increased numbers of Bcl-2–positive cells (Jejurikar et al., 2006). In contrast, the proapoptotic factor Bax is increased in satellite cells of old rat muscle (Krajnak et al., 2006). Therefore, in old muscle, apoptosis may play a causative role in the depletion of satellite cells, impairing the regenerative response to injury.

(Cre10 and Cre 100, respectively). (G) Cre, *dicer*, myogenic marker, and miRNA expression were compared between control *dicer*$^{fl/fl}$ myoblasts infected with adenovirus lacZ expression vector and infected with adenovirus Cre/EGFP expression vector by RT-PCR. For miRNAs, all PCR products are ∼90-bp long. (H) ChIP assay with antibody against RNA polymerase II was performed. Input denotes each PCR product from naked myoblast genomic DNA. Pax3 and Pax7 but not Ig heavy chain (IgH) were detected by ChIP assay in wild-type (wt) and *MyoD*$^{-/-}$ myoblasts. (B and G) β-Actin was monitored as a loading control. *, $P < 0.05$; **, $P < 0.01$. Error bars indicate SEM. Bars, 20 µm.

Downloaded from http://rupress.org/jcb/article-pdf/191/2/347/1869953/jcb_201006025.pdf by guest on 06 December 2025

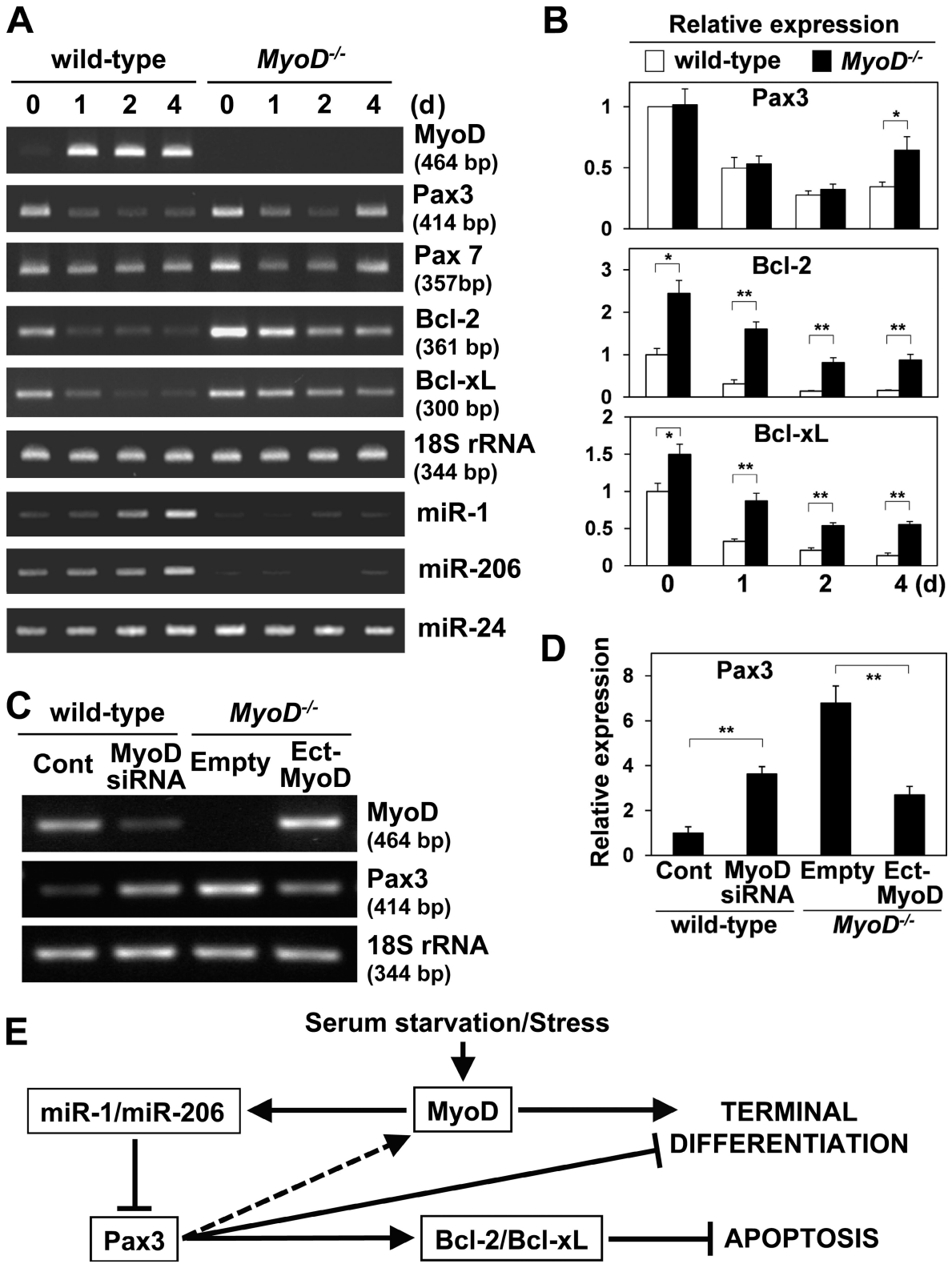

Figure 10. **Pax3 expression is down-regulated during satellite cell activation.** (A) MyoD, Pax3, Pax7, Bcl-2, Bcl-xL, miR-1, and miR-206 gene expression were compared between freshly isolated (day 0) and cultured satellite cells (days 1, 2, and 4) derived from wild-type and *MyoD*$^{-/-}$ mice by RT-PCR. 18S rRNA and miR-24 were monitored as loading controls. For miRNAs, all PCR products are ~90-bp long. (B) Relative Pax3, Bcl-2, and Bcl-xL gene expression levels shown in A normalized by 18S rRNA expression were measured. (C) MyoD and Pax3 gene expression were compared between wild-type satellite cells transfected with siRNA for MyoD and a control siRNA (Cont) or *MyoD*$^{-/-}$ satellite cells infected with a lentivirus vector expressing MyoD (Ect-MyoD) and a control empty vector by RT-PCR. (D) Relative Pax3 gene expression shown in C normalized by 18S rRNA expression was measured. (E) The model for apoptotic cascade regulated by MyoD. MyoD is a master regulator for muscle differentiation. Under differentiation or stressful conditions, MyoD transcriptionally activates miR-1 and miR-206 gene expression, which suppresses Pax3 expression. Down-regulation of Pax3 results in down-regulation of Bcl-2 and Bcl-xL, which causes apoptosis. In addition, down-regulation of Pax3 by MyoD also induces muscle differentiation. *, $P < 0.05$; **, $P < 0.01$. Error bars indicate SEM.

Downloaded from http://rupress.org/jcb/article-pdf/191/2/347/1869953/jcb_201006025.pdf by guest on 06 December 2025

In this study, we demonstrate that MyoD negatively regulates Bcl-2 and Bcl-xL gene expression through down-regulation of Pax3 in satellite cell–derived myoblasts. This cascade might also be involved in aging-related and pathological satellite cell apoptosis during muscle regeneration. X-linked inhibitor of apoptosis protein was reported as an inhibitor for myotube apoptosis, which occurs normally in muscle development, aging, and neuromuscular diseases (Potts et al., 2005; Smith et al., 2009). However, x-linked inhibitor of apoptosis protein expression was not significantly changed between wild-type and *MyoD*$^{-/-}$ myoblasts.

Experiments from gene knockout mice demonstrate that Pax3 functions as survival factors during embryogenesis (Borycki et al., 1999; Pani et al., 2002). It has been reported that Pax3 positively regulates Bcl-xL gene expression by binding to the 5′ flanking region of the Bcl-xL gene (Margue et al., 2000). Previously, screening of binding proteins for the 1 kb Bcl-2 promoter identified 43 different transcription factors including Pax3 (Li et al., 2007). We demonstrate that Pax3 positively regulates Bcl-2 gene expression via the 5′ flanking region of this gene, strongly indicating that Pax3 functions as an antiapoptotic factor by transcriptionally up-regulating Bcl-2 and Bcl-xL gene expression. Pax3 also facilitates the malignant progression of rhabdomyosarcomas and melanomas (Blake and Ziman, 2003; Robson et al., 2006). Pax3 expression is subject to posttranscriptional regulation. Timely down-regulation of Pax3 protein is crucial for myogenic differentiation. Recent work demonstrates that Pax3 expression is regulated by multiple stages, including ubiquitination-mediated protein degradation (Boutet et al., 2007), Staufen 1–mediated mRNA decay (Gong et al., 2009), and miR-27b–mediated translational inhibition (Crist et al., 2009). We have demonstrated that MyoD negatively regulates Pax3 gene expression through the action of miRNAs. Because Pax3 functions as a cell fate determination factor and for maintenance of the undifferentiated state in muscle and melanocyte stem cells, down-regulation of Pax3 is essential for the terminal differentiation, which is also accompanied by apoptosis. Overexpression of MyoD or inhibition of Pax3 by miRNAs may induce apoptosis in rhabdomyosarcomas and melanoma cells, which may provide a novel anticancer therapy for associated tumors (Bernasconi et al., 1996; He et al., 2005).

Previous work has demonstrated that MyoD utilizes miRNAs, including miR-1 and miR-206, to suppress downstream gene expression (Chen et al., 2006; Rosenberg et al., 2006). We have demonstrated that miR-1 and miR-206 bind to two miR-1/miR-206–binding sequences within Pax3-3′UTR and suppress Pax3 expression. We showed that Pax3 expression increases cell survival and suppresses myogenic differentiation in myoblasts. In contrast, miR-1 or miR-206 expression increases cell death and myogenic differentiation. Therefore, down-regulation of Pax3 is required for proper myogenic differentiation, which also results in increased apoptosis. These results are very similar to Pax7, which is involved in maintaining proliferation, preventing precocious differentiation, and protecting against apoptosis (Relaix et al., 2006; Zammit et al., 2006; Olguin et al., 2007). Recently, miR-1 and miR-206 have been shown to act as potent tumor suppressor genes, which inhibit c-met expression in rhabdomyosarcomas (Taulli et al., 2009). Expression of miR-1 or miR-206 in these tumors promotes myogenic differentiation and blocks tumor growth, potentially through inhibition of Pax3 expression. Reduced muscle miRNAs in muscle-specific *dicer* gene knockout mice results in perinatal death and decreased skeletal muscle mass accompanied by abnormal myofiber morphology, indicating the essential role for *dicer* gene in normal muscle development during embryogenesis (O'Rourke et al., 2007). We showed that *dicer* gene knockout myoblasts up-regulated Pax3 gene expression, indicating that the Pax3 gene is regulated by miRNAs. In addition, several muscle specific genes are down-regulated in the *dicer* gene knockout myoblasts, suggesting that *dicer* gene knockout may change broader gene expression in myoblasts, causing the muscle phenotypes seen in the *dicer* gene knockout mice.

Recent work demonstrates that freshly isolated satellite cells but not cultured satellite cells contribute remarkably to muscle fiber regeneration after intramuscular transplantation (Collins et al., 2005; Montarras et al., 2005; Cerletti et al., 2008; Sacco et al., 2008; Tanaka et al., 2009). Freshly isolated satellite cells do not express MyoD until activation (Cornelison et al., 2000). Instead, these cells express Pax3 (Montarras et al., 2005; Boutet et al., 2007), Bcl-2, and Bcl-xL (this study), but expression is quickly down-regulated after activation. Therefore, the QSC population may possess more resistance to apoptosis than ASCs. The down-regulation of MyoD and up-regulation of Pax3 may also be required for maintenance of self-renewing satellite cells. For clinical purposes, myogenic progenitor cells with either suppressed proapoptotic genes such as *MyoD* or miR-1/miR-206 or with forced expression of Pax3 could be screened for their potential to efficiently engraft in damaged muscle, effectively contribute to muscle fiber regeneration, and systemically improve muscle function in muscular dystrophy patients. In addition, these genetically engineered myogenic progenitor cells would be beneficial for therapy by providing a selective advantage in the expansion of muscle stem cells.

Materials and methods

Animals

MyoD$^{-/-}$ mice (Rudnicki et al., 1992) were provided by M.A. Rudnicki (Ottawa Health Research Institute, Ottawa, Ontario, Canada). *MyoD*$^{-/-}$ mice and wild-type mice were used for isolation of *MyoD*$^{-/-}$ and wild-type primary myoblasts. *Rosa26* (Zambrowicz et al., 1997) and *dicer*$^{fl/fl}$ mice (Harfe et al., 2005) were purchased from The Jackson Laboratory. *Nod/Scid*-immunodeficient mice were purchase from Charles River. *MyoD*$^{-/-}$*: Rosa26* mice were established by crossing *MyoD*$^{-/-}$ *mice* with *Rosa26* mice. Genotyping to detect the mutated alleles of *MyoD*$^{-/-}$ and *Rosa26* mice was performed by PCR using primers described by The Jackson Laboratory. Genotyping to detect the *floxed dicer* alleles of *dicer*$^{fl/fl}$ mice was performed by PCR using primers (*floxed dicer* forward and reverse) indicated in Fig. S1. All protocols were approved by the Animal Care and Use Committee of the University of Minnesota.

FACS

QSCs were isolated from the hind limb skeletal muscle of 1–2-mo-old mice after muscle digestion with collagenase type B and dispase II (Roche; Asakura et al., 2002). FACS was performed on an FACS sorter equipped with triple lasers (Aria; BD). The following antibodies were used for FACS sorting: integrin-α7 (MBL International) with Alexa Fluor 488–labeled anti–mouse IgG, biotin-labeled integrin-β1 with allophycocyanin (APC)-labeled avidin, phycoerythrin (PE)-labeled CD45, PE-labeled CD31, and PE-labeled Sca-1 (all obtained from BD; Kuang et al., 2007). Mouse and

Downloaded from http://rupress.org/jcb/article-pdf/191/2/347/1869953/jcb_201006025.pdf by guest on 06 December 2025

rat normal IgG (BD) were used in the control experiment. Alexa Fluor 488 and PE were excited by a 488-nm argon laser, and their fluorescence was detected with an FL1 (530/30) or FL2 (576/26) filter, respectively. APC was excited by a 633-nm red diode laser for the detection with an FL4 filter (620/20). Sorting gates were strictly defined based on single antibody–stained control cells and the forward scatter and side scatter patterns of satellite cells. After the forward scatter/side scatter gating, the triple-negative cells for CD45-PE, CD31-PE, and Sca-1-PE were gated out. Lastly, double-positive cells for integrin-α7 Alexa Fluor 488 and integrin-β1 APC were sorted to enrich for QSCs (Kuang et al., 2007). Sorted QSCs were immediately characterized by immunostaining on slide glasses or cultured on collagen-coated chamber slides (Thermo Fisher Scientific) in the myoblast growth medium to obtain ASCs.

Cell cultures

Satellite cell–derived myoblasts were isolated from the hind limbs of 2-mo-old wild-type BALB/c and *MyoD*$^{-/-}$ mice by FACS (Hirai et al., 2010). The myoblasts were maintained on collagen-coated dishes in myoblast growth medium (Asakura et al., 2001) consisting of HAM's F-10 medium supplemented with 20% FBS and 5 ng/ml basic FGF (R&D Systems). Cell cultures were maintained in a humidified incubator at 37°C with 5% CO_2 and 5% O_2. To induce differentiation of myoblasts, the culture medium was replaced with differentiation medium that contained DME supplemented with 5% horse serum on day 0. The cells were both harvested from day 0 (immediately before switching to the differentiation medium) to day 5 for Western blotting and also fixed with 2% formaldehyde for immunostaining. The medium was changed daily, and cultures were routinely passaged as they reached 60–70% confluence. To ensure that the muscle cells retained physiological characteristics, all experiments were performed using cells that had been passaged between four and eight times.

Intramuscular injection of myoblasts

Muscle regeneration was induced in TA muscle of adult *Nod/Scid* mice by injection of 50 µl 10 µM CTX (Latoxan; Asakura et al., 2002). 1 d later, *Rosa26-* or *MyoD*$^{-/-}$*:Rosa26* myoblasts (10^6 cells) were injected into regenerating TA muscle. 2 d after injection of cells, TA muscles were harvested and stained with x-gal as described previously (Asakura et al., 2002), and 8-µm frozen sections were prepared for immunohistochemistry.

Immunostaining for muscle sections

After x-gal staining of TA muscle sections, TUNEL staining (Promega) was performed following the manufacturer's instructions. Anti-Pax7 antibody (Developmental Biology Hybridoma Bank) followed by Alexa Fluor 488–conjugated anti–mouse IgG secondary antibody (Invitrogen) was used for immunostaining to detect apoptosis in myogenic precursor cells. To detect apoptosis in engrafted myogenic precursor cells, lacZ-stained TA muscle sections were incubated with anti-Pax7 antibody and anti–activated caspase-3 antibody (Abcam) followed by Alexa Fluor 488–conjugated anti–mouse IgG and Alexa Fluor 594–conjugated anti–rabbit secondary antibodies (Invitrogen) for double immunostaining. DAPI (Sigma-Aldrich) was used for counterstaining of nuclei. Fluorescence images were captured using a digital camera (DP-1) attached to an inverted fluorescence microscope (CKX31) with 20× and 40× LUCPlanFLN objectives and a fluorescence microscope (BX51) with 20× and 40× UPlanFLN objectives (all obtained from Olympus). Photoshop (version 7.0; Adobe) was used for image processing.

Immunological staining for cell culture

Immunostaining was performed with an anti-sarcomeric MHC (MF20; Developmental Studies Hybridoma Bank), anti-MyoD antibody (Ab-1; Thermo Fisher Scientific), anti-Pax3 antibodies (Developmental Studies Hybridoma Bank and EMD), anti-Pax7 antibody, and anti–c-met antibody (Santa Cruz Biotechnology, Inc.) followed by Alexa Fluor 488–conjugated anti–mouse IgG antibody (Invitrogen). For Pax3 staining, the TSA kit (Invitrogen) was used for fluorescence signal amplification. Cell cultures were also nuclear stained with DAPI.

Gene KD

MyoD siRNA (Santa Cruz Biotechnology, Inc.), Pax3 siRNA (Santa Cruz Biotechnology, Inc.), and control siRNA-A (Santa Cruz Biotechnology, Inc.) were transfected in wild-type or *MyoD*$^{-/-}$ myoblasts by Lipofectamine 2000 (Invitrogen) following the manufacturer's instructions. A lentivirus-derived shRNA vector for MyoD KD was also created in our laboratory. Short hairpin loops for the lentivirus shRNA were designed according to BLOCK-iT RNAi Designer (Invitrogen), and the vector plasmids were constructed using the BLOCK-iT Lentiviral RNAi Expression System (Invitrogen) according to the manufacturer's instructions. The following oligonucleotides were used for lentivirus vectors expressing two different shRNAs for MyoD: (top strand) 5′-CACCGCTACGACACCGCCTACTACACGAATGTAGTAGGCGGTGTCGTAGC-3′ and (bottom strand) 5′-AAAAGCTACGACACCGCCTACTACATTCGTGTAGTAGGCGGTGTCGTAGC-3′ or (top strand) 5′-CACCGCAAGCGCAAGACCACCAACGCGAACGTTGGTGGTCTTGCGCTTGC-3′ and (bottom strand) 5′-AAAAGCAAGCGCAAGACCACCAACGTTCGCGTTGGTGGTCTTGCGCTTGC-3′. The target sequence for MyoD shRNA is 5′-GCTACGACACCGCCTACTACA-3′ and 5′-GCAAGCGCAAGACCACCAACG-3′. The following oligonucleotides were used for a control lentivirus vector expressing shRNA for GFP: (top strand) 5′-CACCGCTTGGGTGGAGAGGCTATTCCGAAGAATAGCCTCTCCACCCAAGC-3′ and (bottom strand) 5′-AAAAGCTTGGGTGGAGAGGCTATTCTTCGGAATAGCCTCTCCACCCAAGC-3′. The target sequence for control shRNA is 5′-GCTTGGGTGGAGAGGCTATTC-3′. Lentivirus vectors expressing shRNA for MyoD or GFP as a control were transfected into 293T cell lines, and the culture supernatant was used for infection experiments. For MyoD KD, culture supernatant derived from cells transfected with two different lentivirus vectors were mixed and used for infection into myoblasts at the same time. Infection with the lentivirus vectors was performed every day for 3 d. 1 d after final infection, cells were harvested for gene expression and assessed by RT-PCR, immunohistochemistry, and Western blotting or examined for apoptosis assays.

Plasmid vector construction

A retrovirus vector pMX-Pax3 carrying the CMV promoter driving the mouse Pax3 gene was used for Pax3 overexpression experiments. Pax3 cDNA was inserted into the pMXs retrovirus vector (Kitamura et al., 2003). Luc reporter genes conjugating with the mouse Pax3-3′UTR were created from the backbone of pGL3 control vector (Promega), which contains SV40 enhancer/promoter-driving Luc gene. For pLuc-3′UTR and pMX-Pax3-3′UTR, the Pax3-3′UTR fragment (1,225 bp) was amplified by RT-PCR using Platinum Pfx polymerase (Invitrogen), Pax3-E3 forward primer (5′-CATATTGGACAAAAGGCAGGGGAG-3′), and Pax3-E4 reverse primer (5′-ATGTCTCCTGTTCCATCACCCTGC-3′). Total RNA isolated from *MyoD*$^{-/-}$ myoblasts was used for this RT-PCR. The amplified fragments were cloned into pCR2.1-TOPO vector (Invitrogen). The XbaI–SpeI fragment containing the Pax3-3′UTR from the vector was inserted into 3′-XbaI site of the pGL3 control vector and the pMX-Pax3 vector. For mutant genes (pLuc-3′UTRM and pMX-Pax3-3′UTRM), three separated fragments of the 3′UTR were amplified by PCR using Pfx polymerase, M13 reverse (5′-CAGGAAACAGCTATGAC-3′) with Pax3-M1R (5′-CACACACGGATCCTTTTAGCTTCTTTGATC-3′), and Pax3-M1F (5′-GATCAAAGAAGCTAAAAGGATCCGTGTGTG-3′) with Pax3-M2R (5′-AAATCTAAAGGGATCCTATTTGTGCCTACC-3′), Pax3-M2F (5′-GGTAGGCACAAATAGGATCCCTTTAGATTT-3′), and T7 (5′-TAATACGACTCACTATAGGG-3′) primers. The Pax3-3′UTR fragment was used for template DNA. Underlined sequences indicate introduced mutations for the M1 miR-1/miR-206–binding site at Pax3-M1F and Pax3-M1R primers and for the M2 miR-1/miR-206–binding site at Pax3-M2F and Pax3-M2R primers. These three DNA fragments were mixed together and used for a second round of PCR using Pfx polymerase. For this PCR, M13 reverse and T7 primers were used to generate the Pax3-3′UTR with mutations at two miR-1/miR-206–binding sites. The amplified fragments were digested with XbaI and SpeI and inserted into the 3′-XbaI site of the pGL3 control and pMX-Pax3 vectors. For the Bcl-2–Luc reporter gene, genomic PCR was performed using Platinum Pfx polymerase, Bcl-2 F1 primer (5′-CTTCACCCAAGGGTAGCATATTGG-3′), and Bcl-2 R1 primer (5′-AGCAGCTTGCTAAATGCAGGCACG-3′) to amplify the 1,178-bp 5′-flanking region of the mouse Bcl-2 gene. This region is a homologous 5′-flanking region of the rat Bcl-2 gene used for the Bcl-2–P1-Luc reporter plasmid with high Luc activity (Li et al., 2007). Mouse tail DNA was used for the template. Amplified fragments were cloned into pCR2.1-TOPO vector. The XhoI–SacI fragment containing the Bcl-2 upstream region from this vector was inserted into 5′-XhoI–SacI sites of the pGL3 basic vector (Promega).

Virus vector infection

A lentivirus vector pCS2-EF-MyoD carrying the EF1 α-promoter driving the mouse MyoD gene was used for MyoD overexpression experiments as previously described (Asakura et al., 2007). pMXs and pMX-Pax3 retrovirus vectors were transfected into Plat-E retrovirus-producing cells by Lipofectamine 2000 following the manufacturer's instructions. MyoD and Pax3 expression were assessed by RT-PCR, immunohistochemistry, and Western blotting. Adenovirus vectors expressing Cre recombinase and EGFP fusion gene (provided by Y. Kawakami) were used for deletion of *floxed dicer* gene in *dicer*$^{fl/fl}$ myoblasts. The PCR primers (*dicer* del forward and reverse) described in Fig. S1 were used for detection of *dicer* gene after Cre

Downloaded from http://rupress.org/jcb/article-pdf/191/2/347/1869953/jcb_201006025.pdf by guest on 06 December 2025

recombinase expression. All protocols were approved by the Institutional Biosafety Committee of the University of Minnesota.

Semiquantitative RT-PCR

Total RNA was isolated from cells and tissues by TRIzol (Invitrogen). Purified RNA was reverse transcribed (Transcriptor First Strand cDNA Synthesis kit; Roche), and 20–35 PCR cycles were performed (thermal cycler; Eppendorf) using the gene-specific primer pairs described in Fig. S1. Optimal PCR cycles for each pair were determined by several different amplifications of the PCR products. Semiquantitative analysis after RT-PCR was performed using ImageJ software (National Institutes of Health). Each relative expression was calculated by internal control β-actin gene or 18S ribosomal RNA gene expression.

miRNAs

Myoblasts were transfected with pre-miRNA negative control, pre-hsa–miR-1, pre-hsa–miR-206, anti–miR-1, or anti–miR-206 (Applied Biosystems) using Lipofectamine 2000 following the manufacturer's instructions. Transfections were performed three times every day to obtain the maximum gene suppression effect. 1 d after the final transfection, total RNA or protein was isolated for RT-PCR or Western blotting. For differentiation assays, 1 d after final transfection, cells were treated with differentiation medium for an additional 1, 2, or 3 d. For detection of miRNAs, total RNA was isolated from cells by TRIzol (Invitrogen). miRNAs were detected by the mirVana quantitative RT-PCR miRNA detection kit with mirVana PCR primer sets for hsa–miR-1, hsa–miR-15a, hsa–miR-16, hsa–miR-22, hsa–miR-24, hsa–miR-27b, hsa–miR-100, hsa–miR-133a, hsa–miR-191, or hsa–miR-206 in accordance with the manufacturer's instructions (Applied Biosystems). In brief, semiquantitative RT-PCR was performed with miR-specific RT primers followed by 20–35 PCR cycles (thermal cycler; Eppendorf). Optimal PCR cycles for each pair were determined by several different amplifications of the PCR products (~90 bp). TargetScan 4.1 algorithm (http://www.targetscan.org/vert_40/) was used to identify several miRNAs that are predicted to bind to sites on Pax3 mRNA.

Luc reporter assays

The firefly Luc reporter genes pGL3-control, pGL3-basic, pBcl-xL–Luc, pLuc-Pax3-3′UTR, pLuc-Pax3-3′UTR-Mut, and pBcl-xL–Luc (pGL3-6-2; provided by B.W. Schäfer, University Children's Hospital Zurich, Zurich, Switzerland; Margue et al., 2000) were used in this study. pRL-TK (Promega) was used as an internal control. Myoblasts were transfected with pre-miRNAs, MyoD expression vector (pcDNA-MyoD), Pax3 (pcDNA-Pax3) or Pax7 (pcDNA-Pax7), and the Luc reporter genes with Lipofectamine 2000. Cells were harvested at 2 d after transfection. Luc activity was measured with a plate reader (LD400; Beckman Coulter) using a dual Luc reporter assay system (Promega).

Cell fractionation and Western blotting

Mitochondrial and cytosolic proteins were isolated with ApoAlert Cell Fractionation kit (Takara Bio Inc.) following the manufacturer's recommended protocols. Protein concentration of the fractions was determined using the Micro BCA Protein Assay Reagent kit (Thermo Fisher Scientific). Cyt *c* was detected by Western blotting with anti–Cyt *c* antibody (Takara Bio Inc.) followed by anti–rabbit IgG HRP (Cell Signaling Technology). To verify equal loading proteins, the same blots were stripped and reprobed with anti–β-actin antibody (Sigma-Aldrich) as a cytosolic marker or anti–Cyt *c* oxidase subunit IV (COX4) antibody (Takara Bio Inc.) as a mitochondrial marker followed by anti–mouse IgG HRP (Bio-Rad Laboratories). Western blotting was also performed with anti-MyoD antibody (Ab-1; Thermo Fisher Scientific), anti-Pax3 antibody (Developmental Studies Hybridoma Bank), anti-Bcl-2 antibody (Ab-4; Thermo Fisher Scientific), anti–Bcl-xL antibody (Ab-2; Thermo Fisher Scientific), and anti-Bak antibody (Thermo Fisher Scientific). To verify equal loading proteins, the same blots were stripped and reprobed with anti–β-actin or anti–β-tubulin antibody (Sigma-Aldrich). The reaction was developed using SuperSignal West Femto chemiluminescent substrate (Thermo Fisher Scientific) in accordance with the manufacturer's instructions.

Apoptosis assays

For detection of apoptosis, TUNEL assays were performed after UV exposure, treatment with thapsigargin, or low-serum differentiation conditions (DME supplemented with 5% horse serum) using the DeadEnd Colorimetric TUNEL system (Promega) in accordance with the manufacturer's instructions. For differentiation, myoblasts were cultured in low-serum medium without changing medium until 5 d. Dead cell numbers were assessed under the microscope after Trypan blue staining (Invitrogen). The activity of caspase-3 was determined using the CaspACE Assay system (Promega) in accordance with the manufacturer's instructions. The absorbance at 405 nm was determined using a spectrophotometer (Ultrospec 2100 pro; GE Healthcare). Experiments were performed within the linear range of the assay, and absorbance was normalized by the protein concentration of each lysate as determined using the Micro BCA Protein Assay Reagent kit.

ChIP assay

ChIP assay was performed for myoblast cultures using the ChIP assay kit following the manufacturer's instructions (Millipore; Filippova et al., 2001). IP was performed overnight at 4°C with anti–RNA polymerase II (Millipore). PCR primers, Pax3-IP, Pax7-IP, and Ig heavy chain IP used for this assay are described in Fig. S1.

Statistics

All data are expressed as mean ± SEM. Statistical significance between groups was analyzed by Student's *t* test. At least three independent experiments were performed. Asterisk and double asterisk indicate experimental pairs where differences between the compared values were statistically significant ($P < 0.05$ and $P < 0.01$, respectively).

Online supplemental material

Fig. S1 summarizes the list of primer pairs used for RT-PCR experiments. Fig. S2 shows MyoD-dependent apoptosis in myoblasts. Fig. S3 shows gene expression of anti- and proapoptotic genes. Fig. S4 shows that the ectopic expression of Pax3 suppresses muscle differentiation, whereas transfection of miR-1/miR-206 enhances muscle differentiation. Fig. S5 shows a comparison of QSCs isolated from wild-type and *MyoD*$^{-/-}$ mice. Online supplemental material is available at http://www.jcb.org/cgi/content/full/jcb.201006025/DC1.

We thank Drs. Michael A. Rudnicki for providing MyoD mutant mice, Nick Somia for providing the lentivirus vector system, Beat W. Schäfer for providing the Bcl-xL–Luc reporter gene, Roderick H. Dashwood for providing the Bcl-2–Luc reporter gene, Toshioln briefamura for providing the pMXs vector and Plat-E cells, and Genya Gekker for technical assistance in the SCI FACS facility. We also thank Dr. Jonathan M.W. Slack and Bryan A. Piras for critical reading of the manuscript.

This work was supported by grants from the Muscular Dystrophy Association, the Nash Avery Foundation, and the Marzolf Award.

Submitted: 3 June 2010
Accepted: 16 September 2010

References

Asakura, A., and S.J. Tapscott. 1998. Apoptosis of epaxial myotome in Danforth's short-tail (Sd) mice in somites that form following notochord degeneration. *Dev. Biol.* 203:276–289. doi:10.1006/dbio.1998.9050

Asakura, A., M. Komaki, and M. Rudnicki. 2001. Muscle satellite cells are multipotential stem cells that exhibit myogenic, osteogenic, and adipogenic differentiation. *Differentiation.* 68:245–253. doi:10.1046/j.1432-0436.2001.680412.x

Asakura, A., P. Seale, A. Girgis-Gabardo, and M.A. Rudnicki. 2002. Myogenic specification of side population cells in skeletal muscle. *J. Cell Biol.* 159:123–134. doi:10.1083/jcb.200202092

Asakura, A., H. Hirai, B. Kablar, S. Morita, J. Ishibashi, B.A. Piras, A.J. Christ, M. Verma, K.A. Vineretsky, and M.A. Rudnicki. 2007. Increased survival of muscle stem cells lacking the MyoD gene after transplantation into regenerating skeletal muscle. *Proc. Natl. Acad. Sci. USA.* 104:16552–16557. doi:10.1073/pnas.0708145104

Barber, T.D., M.C. Barber, T.E. Cloutier, and T.B. Friedman. 1999. PAX3 gene structure, alternative splicing and evolution. *Gene.* 237:311–319. doi:10.1016/S0378-1119(99)00339-X

Bernasconi, M., A. Remppis, W.J. Fredericks, F.J. Rauscher III, and B.W. Schäfer. 1996. Induction of apoptosis in rhabdomyosarcoma cells through down-regulation of PAX proteins. *Proc. Natl. Acad. Sci. USA.* 93:13164–13169. doi:10.1073/pnas.93.23.13164

Blake, J., and M.R. Ziman. 2003. Aberrant PAX3 and PAX7 expression. A link to the metastatic potential of embryonal rhabdomyosarcoma and cutaneous malignant melanoma? *Histol. Histopathol.* 18:529–539.

Borycki, A.G., J. Li, F. Jin, C.P. Emerson, and J.A. Epstein. 1999. Pax3 functions in cell survival and in pax7 regulation. *Development.* 126:1665–1674.

Boutet, S.C., M.H. Disatnik, L.S. Chan, K. Iori, and T.A. Rando. 2007. Regulation of Pax3 by proteasomal degradation of monoubiquitinated protein in skeletal muscle progenitors. *Cell.* 130:349–362. doi:10.1016/j.cell.2007.05.044

Downloaded from http://rupress.org/jcb/article-pdf/191/2/347/1869953/jcb_201006025.pdf by guest on 06 December 2025

Cerletti, M., S. Jurga, C.A. Witczak, M.F. Hirshman, J.L. Shadrach, L.J. Goodyear, and A.J. Wagers. 2008. Highly efficient, functional engraftment of skeletal muscle stem cells in dystrophic muscles. *Cell.* 134:37–47. doi:10.1016/j.cell.2008.05.049

Chargé, S.B., and M.A. Rudnicki. 2004. Cellular and molecular regulation of muscle regeneration. *Physiol. Rev.* 84:209–238. doi:10.1152/physrev.00019.2003

Chen, J.F., E.M. Mandel, J.M. Thomson, Q. Wu, T.E. Callis, S.M. Hammond, F.L. Conlon, and D.Z. Wang. 2006. The role of microRNA-1 and microRNA-133 in skeletal muscle proliferation and differentiation. *Nat. Genet.* 38:228–233. doi:10.1038/ng1725

Cimmino, A., G.A. Calin, M. Fabbri, M.V. Iorio, M. Ferracin, M. Shimizu, S.E. Wojcik, R.I. Aqeilan, S. Zupo, M. Dono, et al. 2005. miR-15 and miR-16 induce apoptosis by targeting BCL2. *Proc. Natl. Acad. Sci. USA.* 102:13944–13949. doi:10.1073/pnas.0506654102

Collins, C.A. 2006. Satellite cell self-renewal. *Curr. Opin. Pharmacol.* 6:301–306. doi:10.1016/j.coph.2006.01.006

Collins, C.A., I. Olsen, P.S. Zammit, L. Heslop, A. Petrie, T.A. Partridge, and J.E. Morgan. 2005. Stem cell function, self-renewal, and behavioral heterogeneity of cells from the adult muscle satellite cell niche. *Cell.* 122:289–301. doi:10.1016/j.cell.2005.05.010

Cornelison, D.D., B.B. Olwin, M.A. Rudnicki, and B.J. Wold. 2000. MyoD(-/-) satellite cells in single-fiber culture are differentiation defective and MRF4 deficient. *Dev. Biol.* 224:122–137. doi:10.1006/dbio.2000.9682

Crist, C.G., D. Montarras, G. Pallafacchina, D. Rocancourt, A. Cumano, S.J. Conway, and M. Buckingham. 2009. Muscle stem cell behavior is modified by microRNA-27 regulation of Pax3 expression. *Proc. Natl. Acad. Sci. USA.* 106:13383–13387. doi:10.1073/pnas.0900210106

Dee, K., M. Freer, Y. Mei, and C.M. Weyman. 2002. Apoptosis coincident with the differentiation of skeletal myoblasts is delayed by caspase 3 inhibition and abrogated by MEK-independent constitutive Ras signaling. *Cell Death Differ.* 9:209–218. doi:10.1038/sj.cdd.4400930

Dominov, J.A., A.J. Kravetz, M. Ardelt, C.A. Kostek, M.L. Beermann, and J.B. Miller. 2005. Muscle-specific BCL2 expression ameliorates muscle disease in laminin alpha2-deficient, but not in dystrophin-deficient, mice. *Hum. Mol. Genet.* 14:1029–1040. doi:10.1093/hmg/ddi095

Fernando, P., J.F. Kelly, K. Balazsi, R.S. Slack, and L.A. Megeney. 2002. Caspase 3 activity is required for skeletal muscle differentiation. *Proc. Natl. Acad. Sci. USA.* 99:11025–11030. doi:10.1073/pnas.162172899

Fidziańska, A., and H.H. Goebel. 1991. Human ontogenesis. 3. Cell death in fetal muscle. *Acta Neuropathol.* 81:572–577. doi:10.1007/BF00310140

Filippova, G.N., C.P. Thienes, B.H. Penn, D.H. Cho, Y.J. Hu, J.M. Moore, T.R. Klesert, V.V. Lobanenkov, and S.J. Tapscott. 2001. CTCF-binding sites flank CTG/CAG repeats and form a methylation-sensitive insulator at the DM1 locus. *Nat. Genet.* 28:335–343. doi:10.1038/ng570

Fimia, G.M., V. Gottifredi, B. Bellei, M.R. Ricciardi, A. Tafuri, P. Amati, and R. Maione. 1998. The activity of differentiation factors induces apoptosis in polyomavirus large T-expressing myoblasts. *Mol. Biol. Cell.* 9:1449–1463.

Fukada, S., A. Uezumi, M. Ikemoto, S. Masuda, M. Segawa, N. Tanimura, H. Yamamoto, Y. Miyagoe-Suzuki, and S. Takeda. 2007. Molecular signature of quiescent satellite cells in adult skeletal muscle. *Stem Cells.* 25:2448–2459. doi:10.1634/stemcells.2007-0019

Gong, C., Y.K. Kim, C.F. Woeller, Y. Tang, and L.E. Maquat. 2009. SMD and NMD are competitive pathways that contribute to myogenesis: effects on PAX3 and myogenin mRNAs. *Genes Dev.* 23:54–66. doi:10.1101/gad.1717309

Harfe, B.D., M.T. McManus, J.H. Mansfield, E. Hornstein, and C.J. Tabin. 2005. The RNaseIII enzyme Dicer is required for morphogenesis but not patterning of the vertebrate limb. *Proc. Natl. Acad. Sci. USA.* 102:10898–10903. doi:10.1073/pnas.0504834102

Harford, T.J., A. Shaltouki, and C.M. Weyman. 2010. Increased expression of the pro-apoptotic Bcl2 family member PUMA and apoptosis by the muscle regulatory transcription factor MyoD in response to a variety of stimuli. *Apoptosis.* 15:71–82. doi:10.1007/s10495-009-0428-5

He, S.J., G. Stevens, A.W. Braithwaite, and M.R. Eccles. 2005. Transfection of melanoma cells with antisense PAX3 oligonucleotides additively complements cisplatin-induced cytotoxicity. *Mol. Cancer Ther.* 4:996–1003. doi:10.1158/1535-7163.MCT-04-0252

Hirai, H., L. Romanova, S. Kellner, M. Verma, S. Rayner, A. Asakura, and N. Kikyo. 2010. Post-mitotic role of nucleostemin as a promoter of skeletal muscle cell differentiation. *Biochem. Biophys. Res. Commun.* 391:299–304. doi:10.1016/j.bbrc.2009.11.053

Huppertz, B., D.S. Tews, and P. Kaufmann. 2001. Apoptosis and syncytial fusion in human placental trophoblast and skeletal muscle. *Int. Rev. Cytol.* 205:215–253. doi:10.1016/S0074-7696(01)05005-7

Jejurikar, S.S., E.A. Henkelman, P.S. Cederna, C.L. Marcelo, M.G. Urbanchek, and W.M. Kuzon Jr. 2006. Aging increases the susceptibility of skeletal muscle derived satellite cells to apoptosis. *Exp. Gerontol.* 41:828–836. doi:10.1016/j.exger.2006.06.053

Kassar-Duchossoy, L., E. Giacone, B. Gayraud-Morel, A. Jory, D. Gomès, and S. Tajbakhsh. 2005. Pax3/Pax7 mark a novel population of primitive myogenic cells during development. *Genes Dev.* 19:1426–1431. doi:10.1101/gad.345505

Kim, H.K., Y.S. Lee, U. Sivaprasad, A. Malhotra, and A. Dutta. 2006. Muscle-specific microRNA miR-206 promotes muscle differentiation. *J. Cell Biol.* 174:677–687. doi:10.1083/jcb.200603008

Kitamura, T., Y. Koshino, F. Shibata, T. Oki, H. Nakajima, T. Nosaka, and H. Kumagai. 2003. Retrovirus-mediated gene transfer and expression cloning: powerful tools in functional genomics. *Exp. Hematol.* 31:1007–1014.

Krajnak, K., S. Waugh, R. Miller, B. Baker, K. Geronilla, S.E. Alway, and R.G. Cutlip. 2006. Proapoptotic factor Bax is increased in satellite cells in the tibialis anterior muscles of old rats. *Muscle Nerve.* 34:720–730. doi:10.1002/mus.20656

Kuang, S., K. Kuroda, F. Le Grand, and M.A. Rudnicki. 2007. Asymmetric self-renewal and commitment of satellite stem cells in muscle. *Cell.* 129:999–1010. doi:10.1016/j.cell.2007.03.044

Kuwana, T., and D.D. Newmeyer. 2003. Bcl-2-family proteins and the role of mitochondria in apoptosis. *Curr. Opin. Cell Biol.* 15:691–699. doi:10.1016/j.ceb.2003.10.004

Li, Q., W.M. Dashwood, X. Zhong, H. Nakagama, and R.H. Dashwood. 2007. Bcl-2 overexpression in PhIP-induced colon tumors: cloning of the rat Bcl-2 promoter and characterization of a pathway involving beta-catenin, c-Myc and E2F1. *Oncogene.* 26:6194–6202. doi:10.1038/sj.onc.1210438

Margue, C.M., M. Bernasconi, F.G. Barr, and B.W. Schäfer. 2000. Transcriptional modulation of the anti-apoptotic protein BCL-XL by the paired box transcription factors PAX3 and PAX3/FKHR. *Oncogene.* 19:2921–2929. doi:10.1038/sj.onc.1203607

Megeney, L.A., B. Kablar, K. Garrett, J.E. Anderson, and M.A. Rudnicki. 1996. MyoD is required for myogenic stem cell function in adult skeletal muscle. *Genes Dev.* 10:1173–1183. doi:10.1101/gad.10.10.1173

Montarras, D., J. Morgan, C. Collins, F. Relaix, S. Zaffran, A. Cumano, T. Partridge, and M. Buckingham. 2005. Direct isolation of satellite cells for skeletal muscle regeneration. *Science.* 309:2064–2067. doi:10.1126/science.1114758

Morishima, N., K. Nakanishi, K. Tsuchiya, T. Shibata, and E. Seiwa. 2004. Translocation of Bim to the endoplasmic reticulum (ER) mediates ER stress signaling for activation of caspase-12 during ER stress-induced apoptosis. *J. Biol. Chem.* 279:50375–50381. doi:10.1074/jbc.M408493200

O'Rourke, J.R., S.A. Georges, H.R. Seay, S.J. Tapscott, M.T. McManus, D.J. Goldhamer, M.S. Swanson, and B.D. Harfe. 2007. Essential role for Dicer during skeletal muscle development. *Dev. Biol.* 311:359–368. doi:10.1016/j.ydbio.2007.08.032

Olguin, H.C., Z. Yang, S.J. Tapscott, and B.B. Olwin. 2007. Reciprocal inhibition between Pax7 and muscle regulatory factors modulates myogenic cell fate determination. *J. Cell Biol.* 177:769–779. doi:10.1083/jcb.200608122

Pani, L., M. Horal, and M.R. Loeken. 2002. Rescue of neural tube defects in Pax-3-deficient embryos by p53 loss of function: implications for Pax-3-dependent development and tumorigenesis. *Genes Dev.* 16:676–680. doi:10.1101/gad.969302

Peschiaroli, A., R. Figliola, L. Coltella, A. Strom, A. Valentini, I. D'Agnano, and R. Maione. 2002. MyoD induces apoptosis in the absence of RB function through a p21(WAF1)-dependent re-localization of cyclin/cdk complexes to the nucleus. *Oncogene.* 21:8114–8127. doi:10.1038/sj.onc.1206010

Potts, M.B., A.E. Vaughn, H. McDonough, C. Patterson, and M. Deshmukh. 2005. Reduced Apaf-1 levels in cardiomyocytes engage strict regulation of apoptosis by endogenous XIAP. *J. Cell Biol.* 171:925–930. doi:10.1083/jcb.200504082

Rao, P.K., R.M. Kumar, M. Farkhondeh, S. Baskerville, and H.F. Lodish. 2006. Myogenic factors that regulate expression of muscle-specific microRNAs. *Proc. Natl. Acad. Sci. USA.* 103:8721–8726. doi:10.1073/pnas.0602831103

Relaix, F., D. Rocancourt, A. Mansouri, and M. Buckingham. 2005. A Pax3/Pax7-dependent population of skeletal muscle progenitor cells. *Nature.* 435:948–953. doi:10.1038/nature03594

Relaix, F., D. Montarras, S. Zaffran, B. Gayraud-Morel, D. Rocancourt, S. Tajbakhsh, A. Mansouri, A. Cumano, and M. Buckingham. 2006. Pax3 and Pax7 have distinct and overlapping functions in adult muscle progenitor cells. *J. Cell Biol.* 172:91–102. doi:10.1083/jcb.200508044

Robson, E.J., S.J. He, and M.R. Eccles. 2006. A PANorama of PAX genes in cancer and development. *Nat. Rev. Cancer.* 6:52–62. doi:10.1038/nrc1778

Rosenberg, M.I., S.A. Georges, A. Asawachaicharn, E. Analau, and S.J. Tapscott. 2006. MyoD inhibits Fstl1 and Utrn expression by inducing transcription of miR-206. *J. Cell Biol.* 175:77–85. doi:10.1083/jcb.200603039

Downloaded from http://rupress.org/jcb/article-pdf/191/2/347/1869953/jcb_201006025.pdf by guest on 06 December 2025

Rudnicki, M.A., T. Braun, S. Hinuma, and R. Jaenisch. 1992. Inactivation of MyoD in mice leads to up-regulation of the myogenic HLH gene Myf-5 and results in apparently normal muscle development. *Cell.* 71:383–390. doi:10.1016/0092-8674(92)90508-A

Sabourin, L.A., A. Girgis-Gabardo, P. Seale, A. Asakura, and M.A. Rudnicki. 1999. Reduced differentiation potential of primary *MyoD*$^{-/-}$ myogenic cells derived from adult skeletal muscle. *J. Cell Biol.* 144:631–643. doi:10.1083/jcb.144.4.631

Sacco, A., R. Doyonnas, P. Kraft, S. Vitorovic, and H.M. Blau. 2008. Self-renewal and expansion of single transplanted muscle stem cells. *Nature.* 456:502–506. doi:10.1038/nature07384

Sandri, M., and U. Carraro. 1999. Apoptosis of skeletal muscles during development and disease. *Int. J. Biochem. Cell Biol.* 31:1373–1390. doi:10.1016/S1357-2725(99)00063-1

Schwartz, L.M., Z. Gao, C. Brown, S.S. Parelkar, and H. Glenn. 2009. Cell death in myoblasts and muscles. *Methods Mol. Biol.* 559:313–332. doi:10.1007/978-1-60327-017-5_22

Smith, M.I., Y.Y. Huang, and M. Deshmukh. 2009. Skeletal muscle differentiation evokes endogenous XIAP to restrict the apoptotic pathway. *PLoS One.* 4:e5097. doi:10.1371/journal.pone.0005097

Tanaka, K.K., J.K. Hall, A.A. Troy, D.D. Cornelison, S.M. Majka, and B.B. Olwin. 2009. Syndecan-4-expressing muscle progenitor cells in the SP engraft as satellite cells during muscle regeneration. *Cell Stem Cell.* 4:217–225. doi:10.1016/j.stem.2009.01.016

Taulli, R., F. Bersani, V. Foglizzo, A. Linari, E. Vigna, M. Ladanyi, T. Tuschl, and C. Ponzetto. 2009. The muscle-specific microRNA miR-206 blocks human rhabdomyosarcoma growth in xenotransplanted mice by promoting myogenic differentiation. *J. Clin. Invest.* 119:2366–2378.

Walsh, K. 1997. Coordinate regulation of cell cycle and apoptosis during myogenesis. *Prog. Cell Cycle Res.* 3:53–58.

Wang, S., and E.N. Olson. 2009. AngiomiRs—key regulators of angiogenesis. *Curr. Opin. Genet. Dev.* 19:205–211. doi:10.1016/j.gde.2009.04.002

Wang, J., and K. Walsh. 1996. Resistance to apoptosis conferred by Cdk inhibitors during myocyte differentiation. *Science.* 273:359–361. doi:10.1126/science.273.5273.359

Weintraub, H., R. Davis, S. Tapscott, M. Thayer, M. Krause, R. Benezra, T.K. Blackwell, D. Turner, R. Rupp, S. Hollenberg, et al. 1991. The myoD gene family: nodal point during specification of the muscle cell lineage. *Science.* 251:761–766. doi:10.1126/science.1846704

White, J.D., A. Scaffidi, M. Davies, J. McGeachie, M.A. Rudnicki, and M.D. Grounds. 2000. Myotube formation is delayed but not prevented in MyoD-deficient skeletal muscle: studies in regenerating whole muscle grafts of adult mice. *J. Histochem. Cytochem.* 48:1531–1544.

Zambrowicz, B.P., A. Imamoto, S. Fiering, L.A. Herzenberg, W.G. Kerr, and P. Soriano. 1997. Disruption of overlapping transcripts in the ROSA beta geo 26 gene trap strain leads to widespread expression of beta-galactosidase in mouse embryos and hematopoietic cells. *Proc. Natl. Acad. Sci. USA.* 94:3789–3794. doi:10.1073/pnas.94.8.3789

Zammit, P.S., L. Heslop, V. Hudon, J.D. Rosenblatt, S. Tajbakhsh, M.E. Buckingham, J.R. Beauchamp, and T.A. Partridge. 2002. Kinetics of myoblast proliferation show that resident satellite cells are competent to fully regenerate skeletal muscle fibers. *Exp. Cell Res.* 281:39–49. doi:10.1006/excr.2002.5653

Zammit, P.S., F. Relaix, Y. Nagata, A.P. Ruiz, C.A. Collins, T.A. Partridge, and J.R. Beauchamp. 2006. Pax7 and myogenic progression in skeletal muscle satellite cells. *J. Cell Sci.* 119:1824–1832. doi:10.1242/jcs.02908

Downloaded from http://rupress.org/jcb/article-pdf/191/2/347/1869953/jcb_201006025.pdf by guest on 06 December 2025